Doctoral Dissertation

Improvement of Long-term Stability of Polypropylene-based Materials through Encapsulation and Morphology Control

by

Ikki Katada

Supervisor: Professor Minoru Terano

School of Materials Science

Japan Advanced Institute of Science and Technology

March 2015

Preface

The present dissertation is the result of the studies under the direction of Professor Dr. Minoru Terano during 2012-2015. The purpose of this dissertation is a basis of the stabilization of polypropylene materials. The fundamentals in the polypropylene chemistry related to degradation and stabilization is presented as a general introduction in the first chapter. Chapter 2 shows the novel stabilization approach of polypropylene materials using hyperbranched polymer. Chapter 3 shows the development of this approach to polypropylene nanocomposites. Chapter 4 shows the effect of dendritic polymer on nano filler surface for stabilization of PP nanocomposites. Chapter 5 shows the control of crystalline unit cell for long-term stabilization on electrical breakdown property. The last chapter summarizes the conclusive items of this dissertation.

Ikki Katada

Terano Laboratory,

School of Materials Science,

Japan Advanced Institute of Technology

Referee-in-chief: **Professor Dr. Minoru Terano**

Japan Advanced Institute of Science and Technology

Referees: **Professor Dr. Masayuki Yamaguchi**

Japan Advanced Institute of Science and Technology

Professor Dr. Noriyoshi Matsumi

Japan Advanced Institute of Science and Technology

Associate Professor Dr. Toshiaki Taniike

Japan Advanced Institute of Science and Technology

Professor Dr. Katsuhisa Tokumitsu

The University of Shiga Prefecture

Contents

Chapter 5. Long-term Stability for Capacitor Applications by Controlling Crystal Morphology

5.1. Introduction

5.2 Experimental Section

5.3. Results and Discussion

5.4. Conclusion

Chapter 6. General conclusion

6.1 General Summary

6.2 Conclusion

Chapter 1

General Introduction

1.1. Polypropylene

1.1.1. Background

High isotactic polypropylene (PP) is widely used plastics and one of the most important materials in the worlds because of its balanced properties. PP recognized that the discovery not only represented the first and most significant step in the synthesis of crystalline PP at the scientific and industrial level. In the years following its discovery, PP went through such a dynamic industrial development that it is one of the most widely used polymeric materials. Ziegler Natta (ZN) catalyst is most widely used for industrial production of 99% of PP and it has been used in numerous applications. As the development of catalyst chemistry has continued, the polymer morphology, properties and reactivity have been improved. Explosive growth of PP is due to the outstanding combination of cost performance, excellent physical properties, processability, and environmental friendly [1].

The application areas of PP also have been expanded with increasing its production amounts. Development of PP materials is still now desired in automobile fields especially because of its processability and so on. The researches of PP materials for accomplishments of its high performances are mainly classified to two classes. One is “Control PP primary structure by catalyst technology”, and the other is “control high order structure by compounding technology”. Recent the most notable breakthrough achievement in the last couple of decades is “Nanocomposite”, which is classified to latter. Details of nanocomposites were indicated in chapter 1.2.

On the other hand, environment-conscious materials are also necessary for the coming century and PP will be expected as one of them. Polylactic acid is the most

desirable materials in environment-conscious materials because of its biodegradability [2]. However, PP materials, which is petrochemical raw materials, have been also tried to be gone as a carbon-neutrals [3,4].

With the rapid growth of PP industry have been needed the emergence of a new grade of general purpose plastics having higher performances. Therefore, the structure and morphology of PP are also introduced in this chapter. And also PP crystalline form is one of the important factors in chapter 4 especially. The explanation of PP structure was focused on.

1.1.2. Crystalline structures of Polypropylene

PP is a semi-crystalline polymer, which the crystalline architecture and crystallization of PP have been topics of interest. It is naturally expected that crystal structure and crystallization behavior are not only dependent upon molecular weight and molecular weight distribution, but also upon tacticities. Figure 1.1.2.1 shows PP chain molecule possesses a chain conformation with a 2 x 3/1 helix (tgtg).

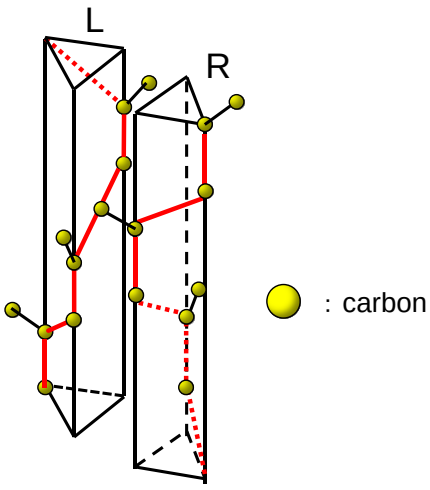

Figure 1.1.2.1. PP chain helix (L) left-handed helix, (R) right-handed helix

PP properties are strongly determined by its crystalline structure, and the relative amount of amorphous and crystalline phases, crystal modification, size and perfection of crystallites, dimensions of spherulites and the number of tie molecules all influence the performance of PP products [5]. Since the presence of the asymmetrically substituted methyl groups causes rotation around the backbone bonds to be direction-dependent, both right-handed and left-handed helices with stereo-isomer configurations of *d* and *l* result [6-10]. Combination of these possibilities leads to four distinguishable chain conformations.

The intramolecular interaction energies of all four types of helices are identical. Their intermolecular interactions with each other in the crystal packing, however, depend upon packing geometry. Best packing is frequently achieved when the nearest neighbors of right-handed helices are the enantiomorphic left-handed helices and vice versa. Different packing geometries lead to four well-known crystal structures (polymorphs). The monoclinic (α) form [11], the hexagonal (β) form [12-14], the triclinic (γ) form [15-17] and the quenched form. Some reports have also proposed the existence of a δ form [18]. Among these crystal structures, the monoclinic (α) form is by far the most common, being formed in normal crystallized PP samples. The unoriented powder wide angle X-ray diffraction (WAXD) patterns for different forms in PP crystals are shown in Figure 1.1.3. Formation of these different forms is critically dependent on crystallization conditions and molecular characteristics. Because my work is especially relating to α form crystal in chapter 4, it was explained in chapter 1.1.3.

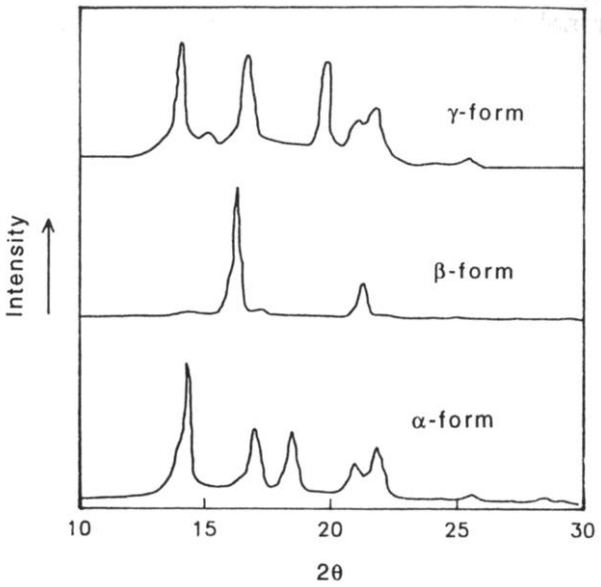

Figure 1.1.3. WAXD patterns for different forms in PP crystals

1.1.3. α form

The crystal unit cell of the α form was reported to be a = 0.666 nm, b = 2.078 nm, c = 0.6495 nm, β = 99.62, and α = γ = 90˚C, with a crystallographic symmetry (space group) of P21/c [19]. The number of repeating unit cell involved in each unit cell is twelve and the crystallographic density is 0.946 g/cm3. Based on the unit cell reported by Natta and Corradini [20], a = 0.665 nm, b = 2.096 nm, c = 0.650 nm, β= 99.33, and α = γ = 90˚C, the crystallographic density of the α form should be 0.936 g/cm^3. It is particularly interesting that the three-fold screw axis of the PP molecule is not part of the crystal symmetry, as shown in Figure 1.1.4.

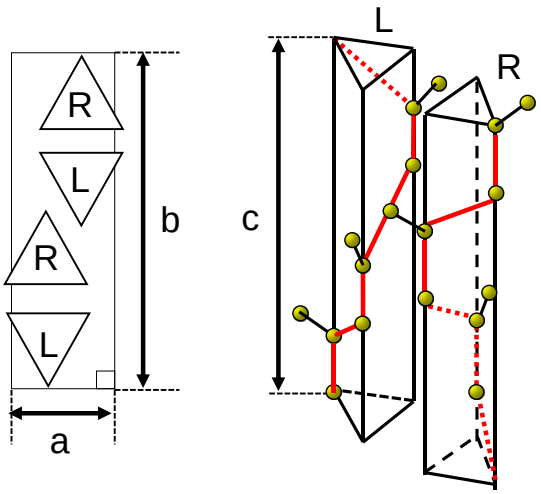

Figure 1.1.4. PP crystal unit cells of α form.

Although only isoclined helices (opposite handedness contacts) are evident here, the α form of PP also has two isomorphic (equal handedness contacts) helices. This leads to an increase in the coordination number without loss of packing by contacting helices of equal handedness. Another important feature lies in the positioning of the methyl groups within the polymer, isoclined (the methyl group is 'up' related to the left glide plane) and anticlined (the methyl group is 'down' related to the left glide plane) or vise versa. This introduces a high degree of disorder in PP crystals. It was reported that the α form in PP can be recrystallized and/or annealed from a less ordered α_1 form with a random distribution of 'up' and 'down' chain packing of methyl groups to a more ordered α_2 form with a well-defined deposition of 'up' and 'down' helices in the crystal unit cell. The packing energy difference between these two forms is only a few tenths of one kJ/mol. The space groups of these two forms are shown in Figure 1.1.5.

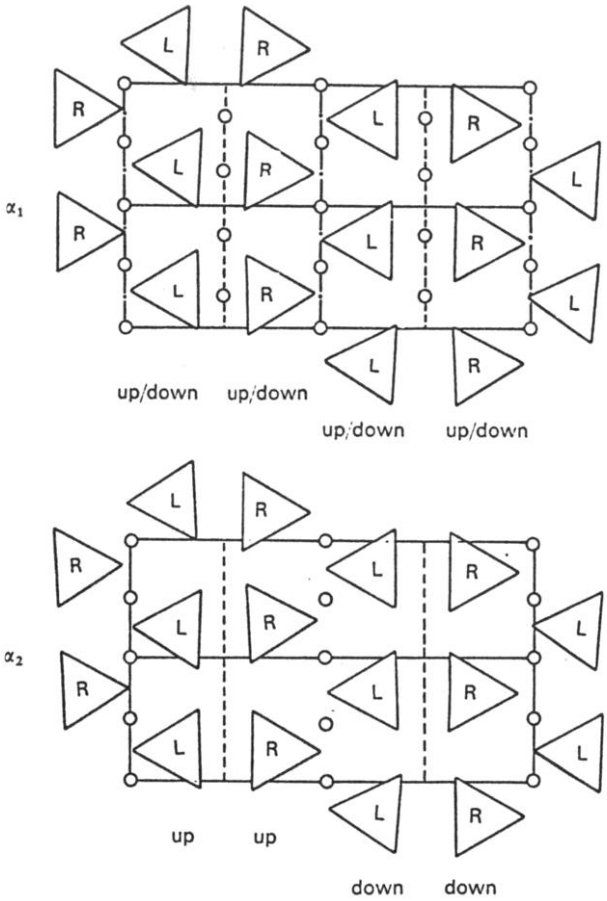

Figure 1.1.5. Two monoclinic space groups, corresponding to α_1 and α_2 forms in PP

The α form is the most common and most extensively studied crystalline structure in PP. As for the lamellar scale, from transmission electron microscopy (TEM) observations, the crystalline morphology of PP is dominated by a highly characteristic lamellar branching (cross-hatch), which has no counterpart in other crystalline polymers [21]. Note that the cross-hatch structure is observed only for the α form, and not for the other forms. It has been recognized that this lamellar branching is formed by a constant angle between daughter (tangential direction in the spherulites) and parent (radial direction in the spherulites) lamellar of 80˚ or 100˚. The degree of the branching is depended on the T_c. and isotacticity. The branching decreases with

isotacticity of PP. In principle, the branching is an epitaxial growth phenomenon. It is explained by mainly three different aspects: molecular, crystallographic and morphological aspects [22]. The most general study was made by Lotz and Wittmann [23]. They suggested that structurally the daughter lamellae in PP grow epitaxially on the lateral (010) crystallographic plane of the parent lamellae by a satisfactory interdigitation of the methyl groups of facing planes. This condition arises from the near identity of the size of the a and c axes in the unit cell of the α form. From a molecular point of view, chains that deposit onto the (010) plane for the initiation of the epitaxy have the same helical handedness as chains in the (010) plane, but with a substantial angle of 80˚ or 100˚ in order to have favorable interactions of the methyl groups in the helices. In this study, 209 J/g was used based on the value from a literature, which seems to be one of the most reliable values [24].

1.2. Polypropylene Based Nanocomposites

1.2.1. Background

The Toyota researchers have developed a clay/nylon nanocomposite with excellent mechanical properties [25,26]. This success has aroused much attention for the use of polymer nanocomposites. The nanocomposite has been used to fabricate parts of automobiles, but this application was stopped because of the high cost. The high cost was caused by the time-intensive preparation process and the high price of nylon. This is why our group has aimed to develop nanocomposites using PP as a matrix.

In order to develop polymer nanocomposites as engineering plastics with high mechanical properties, at least two requirements must be satisfied. One is to separate

the stacked layer structure of clay, into monolayers if possible, in a polymer matrix. The aspect ratio of the filler particle increases and as a result, the reinforcement effects are enhanced [27,28]. Another is to control the interfacial affinity between a clay particle surface and the matrix polymer [29,30]. We also thought that the type of filler would influence the mechanical properties of the resulting nanocomposites. So, spherical nano filler was chosen as filler for PP nanocomposites in our lab to subtract the factor of aspect ratio.

1.2.2. Polypropylene/SiO_2 Nanocomposites

The mechanical properties of PP nanocomposites have been also improved [31] and PP/clay nanocomposite achieved to the application level as industrial fields [32,33].

Generally, non-polar nature of PP structure made PP more difficulty to improve their properties by using conventional techniques than other polar polymers. The developments of new techniques have been highly required for the preparation of PP nanocomposite. The preparation methods and processing work have been led to the development of the nanocomposites. Spherical SiO_2 was also applied as a nano-filler for PP nanocomposites. Among PP-based nanocomposites, PP/SiO_2 nanocomposite is one of the most reported systems from both academic and industrial fields. SiO_2 has been widely used as a reinforcing agent for the rubbery materials. The use of SiO_2 for other polymers like polyolefin is expected because of their price, properties and non-toxic aspects. In 1990, Osseoasare and Arrigada prepared nano-sized and mono-disperse SiO_2 particles by controlled hydrolysis of tetraethoxysilane (TEOS) in an inverse micro emulsion. This micro emulsion method is also widely used to

synthesize SiO_2 nanoparticles. SiO_2 nanoparticles are now available from commercial sources, and they usually exist as powder or colloid.

In the case of PP/SiO_2 nanocomposites, three general methods can be applied according to the starting materials and processing techniques: blending, sol-gel process and in-situ polymerization. Blending is just mixing of SiO_2 nanoparticles into a polymer. For the preparation of SiO_2 nanocomposites, fumed silica is commonly used and precipitated silica is seldom used since the precipitated one has more silanol groups (Si-OH) on the surface and consequently it is much easier to agglomerate than fumed one. As for commercial colloidal SiO_2 spheres, they are usually in the form of a sol with water or alcohol as a dispersing medium. The surface of SiO_2 is typically terminated with three silanol types: free or isolated silanols, hydrogen bonded or vicinal silanols and geminal silanols. Silanol groups residing on adjacent particles form hydrogen bonds and lead to formation of aggregates.

Our previous research got the highest mechanical property in the case of PP/SiO_2 nanocomposites by grafting PP onto SiO_2 surface [34]. Concept of our previous research was shown in Figure 1.2.1. This grafted PP acts as a rule of crystallization factor and this work suggested that co-crystallization between matrix PP and grafted PP might be existed. The highest improvement of PP/SiO_2 nanocomposites may come from reinforcement of interface adhesion, which is weaker than polar nature polymers. And the dispersion of SiO_2 was also improved by grafted PP. Because of the availability of PP nanocomposite, SiO_2 was chosen as nano filler in this research.

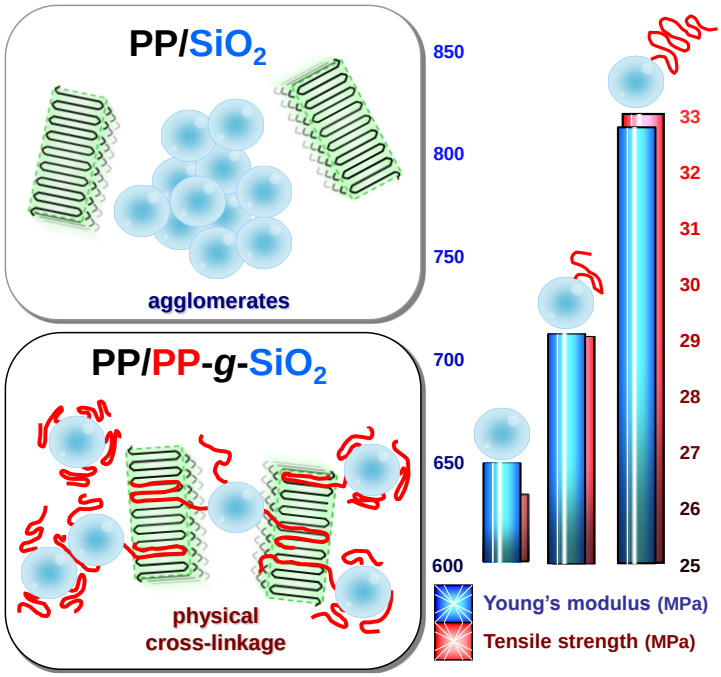

Figure 1.2.1. Results of our previous research

1.3. Degradation and Stabilization

1.3.1 Background

PP is easier to degradate than other polymers because of its tertiary hydrogen contained PP backbone. These tertiary hydrogens, which connect tertiary carbon, have higher radical reactivity and accelerate degradation reaction of PP [35]. However, it is not serious problem for PP application when we use PP as final products. It is known that the stability and lifetime of PP products were decided by the additives like antioxidants. Antioxidants can react with oxygen to substitute for PP itself. While antioxidants are working, PP degradation can be suppressed and PP can keep its good performances. In other words, the most important factor for the PP stability and lifetime is how to use antioxidants.

1.3.2. Degradation

Although PP is well known as a versatile plastic, its degradation is one of the most serious problems. After polymerization, PP is subjected to several processing steps involving extrusions. Even small degree of degradation reaction, it has an enormous effect on the physical properties. Generally it is well known that the degradation can be initiated by oxygen, shear, heat, light, catalyst residues and so on. It is widely accepted that the degradation follows so called 'auto-oxidation mechanism' as shown in Scheme 1.3.1 and Scheme 1.3.2.

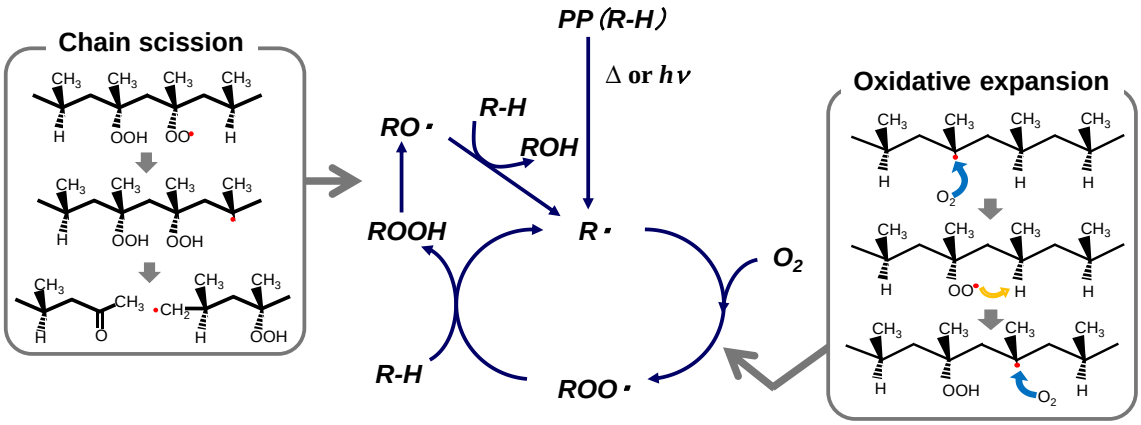

Scheme 1.3.1. Degradation of PP [36]

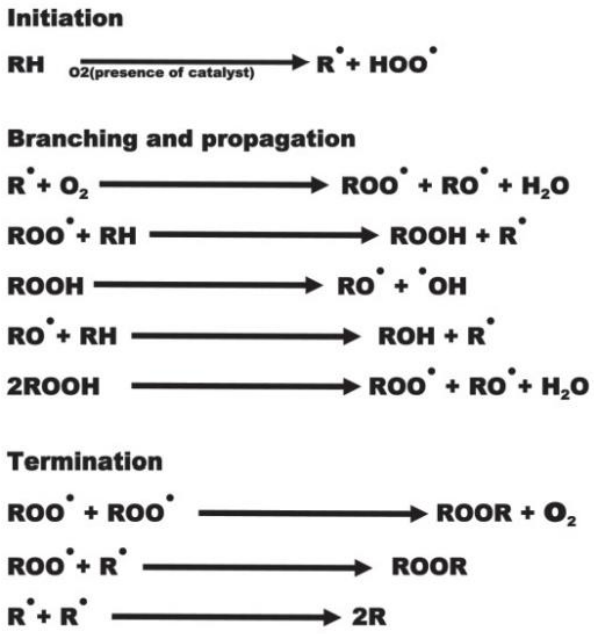

Scheme 1.3.2. Schematic of oxidation reactions [37]

The initiation reactions are still controversial and many factors can contribute to the formation of the first macro-alkyl radicals, e.g. heat, mechanical stress, light and transition metal impurities (catalyst residue. etc.,). Propagation reactions involve the very fast reaction of oxygen (a biradical) with polymer alkyl radicals leading to the formation of macro-alkylperoxyl radicals. This is followed by a slower (rate determining) reaction involving the abstraction of a hydrogen from another polymer molecule giving rise to the formation of macro-hydroperoxides, the first molecular product in the chain reaction; the rate of H-abstraction is a function of both the C-H bond dissociation energy and the stability of the final macro-alkyl radical. Hydroperoxides formed in this reaction are associated with further initiation reactions, resulting in detrimental changes to molar mass and properties of the polymer, ultimately leading to catastrophic failure. The nature of the termination reaction is highly dependent on the molecular structure of the polymer and the prevailing conditions.

For example, under normal oxygen pressure (oxygen saturation), conditions dominating in the course of end-product use, the Hydroperoxide (ROO•) radicals are the predominant reactive species, i.e. [ROO•] > [R•], and termination reactions predominate.

However, in the presence of limited amounts of oxygen (oxygen deficiency), conditions occurring mainly during polymer processing as well as in thick samples where oxidation rate is controlled by oxygen diffusion, alkyl radicals predominate, i.e. [R•] > [ROO•], and bimolecular termination reactions involving R assume greater significance. This leads to polymer cross-linking and increased molar mass, and /or disproportionation without change to molar mass. However, it also accepted that the atmosphere, which contains about 20% of oxygen, with weak flow is enough to saturate reactive oxygen for PP degradation.

For better understanding of PP degradation, a lot of studies were reported relating to the effects of basic characters of PP, such as stereo-regularity, molecular weight, crystallinity (amorphous fraction) etc., on the degradation behavior. Moreover, other factors such as catalyst residue, presence of fillers also affect the degradation. On the other hand, from the point of macroscopic scale, PP degradation occurs heterogeneously from amorphous phase of PP, not from crystalline phase, and it also spatially heterogeneously spreads through the weaker area for the degradation. Degradation behavior of PP has been evaluated by a lot of methods. Spectroscopic measurements like Raman analyses are one of the most frequently used to detect carbonyl or ester compounds and/or carbon double bonds which are made during degradation.

1.3.2. Stabilization

Prevent of polymer degradation has been the most important topic when they were used as products. The additives which prevent polymer degradations and elongate their life-time are called “antioxidant”. These antioxidants can be classified mainly two categories. One is known as a radical scavenger, which traps radicals in polymer chain, and the other is peroxide decomposer, which suppresses to generate new peroxide. The stabilization mechanism is shown in Scheme 1.3.3.

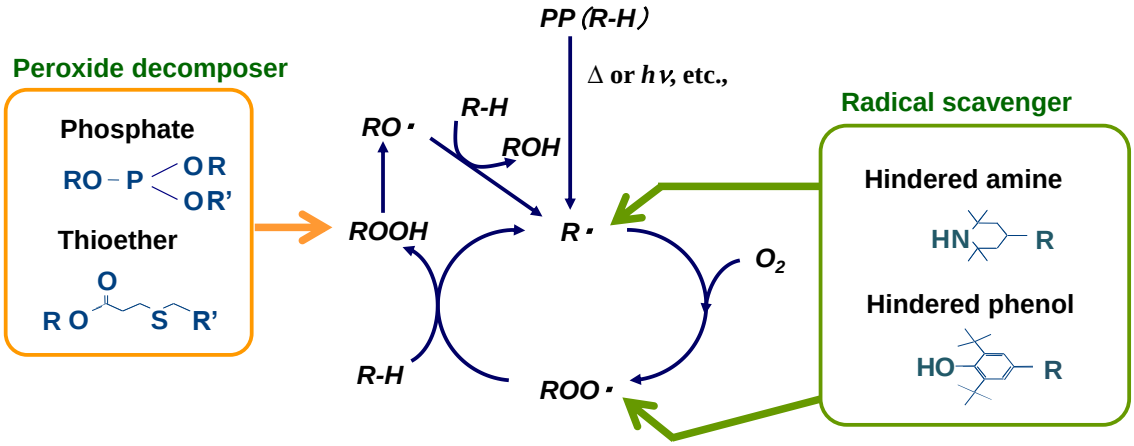

Scheme 1.3.3. Stabilization mechanism by antioxidants

Since PP is very weak for degradation due to the presence of tertiary hydrogen atoms in main chain, products must be stabilized by the addition of various antioxidants for real use.

How to use antioxidants is the most important for the long-term usage of PP. There are two main factors to elongate the lifetime of antioxidants itself when the usage of antioxidants. One is “Chemical loss of antioxidants” and the other is “Physical loss of antioxidants” [38,39]. The former indicates the loss during radical reactions. It is

generally accepted that the one hindered phenol can react two radicals (peroxides). And then antioxidant deactivated itself with suppressing PP degradation. This chemical loss can be controlled by changing the amounts of antioxidants. Otherwise, latter indicates volatilization and dissolution loss of antioxidants from PP matrix without working fully by dissolving and so on. This problem is difficult to be solved because it becomes prominent when we increase the amounts of antioxidants.

From the standpoint of the industrial, blending technics with PP and antioxidants have been mainly developed. For example, coexisting of lower molecular antioxidants and higher molecular one is one of the beneficial methods because it can suppress the volatilization of antioxidants, and keep its diffusion in matrix. In academicals fields, grafting reaction of antioxidants was applied to suppress volatilization and to elongate the life time [40].

UV-vis measurement is also effective to detect remaining antioxidants. Recently many techniques have been developed and extended to two dimensional evaluation coupled with microscopy techniques (as known IR or Raman microscopy analyses), and many reports have reported the heterogeneous degradation behavior.

For the commercial need, other requirements become necessary not only to maintain properties of PP but also to extend its service life. Much more developments of high-performance of the PP materials are highly required, which addresses more stringent or new requirements such as more severe processing and use conditions and/or environmental concerns.

1.3.3. Degradation of Composites

Polymer or PP compounds with other materials, especially inorganic fillers, are one of the most promising technics for the developments as I mentioned. However, the most serious problem is its degradation which prevents their developments because of acceleration of degradation and rarely recyclable ability [41]. To break down the status quo, improvement of antioxidants efficiency in polymer matrix is necessary like in the case of homo PP.

The reason why PP composite is easier to degradate than homo is known as the absorption of antioxidants on filler surface and /or existence of metal ion, which is proceed degradation, and so on[42]. In addition, we reported the degradation behavior of antioxidants in PP/SiO_2 composites. It was observed that the interface between filler and PP matrix got weaker and volatilization of antioxidant was accelerated from this interface [43]. That is to say, the volatilization is also a serious problem that needs to be solved to improve PP compounds properties. Cao et al, reported that grafting reaction of antioxidants on filler surface was useful to elongate polymer life time[44-46].

1.4. Hyperbranched Polymer

Hyperbranched polymers (HBPs) have specific architectures compared with linear polymers. It can also be attractive material for the functionalization of the materials. HBPs are highly branched macromolecules with three-dimensional dendritic architecture. Polymer viscosity is generally increased with increasing its molecular

weight because its entanglements also increase each other. In the case of HBP, the viscosity tends to decrease with increasing their molecular weight. This phenomenon comes from specificity of HBPs. HBP has dendritic structure, which has less chain entanglements. Therefore, the potentials of HBPs expand their application area as not only processing but also medical materials. The architecture of HBP was shown in Figure 1.4.1. Their classification has been defined with their generations.

Due to their unique physical (e.g. low melt viscosity) and chemical (e.g. a large number of functional groups) properties different from linear polymers, they have expected as a new class of materials in various fields such as drug-deliverly, coatings, or additives [47-49].

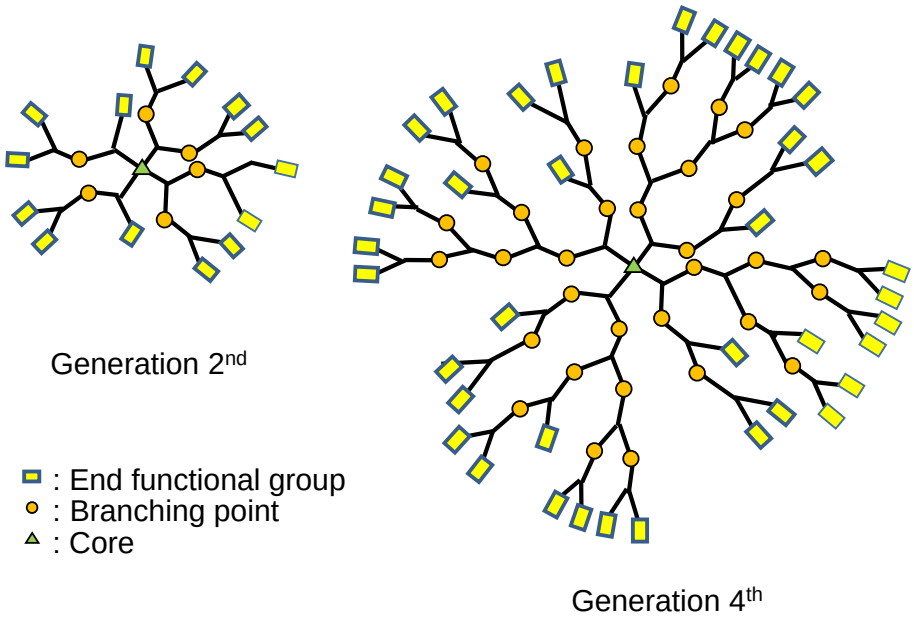

Figure 1.4.1. Architectures of hyperbranched polymer (left) Generation 2nd (right) Generation 4th.

The synthetic development in the field of hyperbranched polymers in the last two decades is based on the fact that these compounds possess new, particular characteristics that strongly influence material properties and open new application fields[50-54].

HBPs and their substitutes can be regarded as nanomaterials because of their molecular size. In particular, many researchers have intensively investigated the use of HBP for host-guest encapsulation and the fabrication of organic-inorganic hybrids.

1.5 Durability of PP in capacitor application

1.5.1 Background

Insulating materials have been used as electrical wiring, cable protectors and so on. Recent developments of transistors and integrated circuits made insulating materials higher performance like plastic films. These developments have been contributed to properties improvements of polymer films which has very thin layer through processing ability.

1.5.2. Capacitor

Insulate materials can keep electrostatic energy. This is like a dam which can keep water. When electrical conductive materials have been directed parallel each other, the electrostatic energy can be kept between them. Capacitors are one of these applications. The principle shows in Figure 1.5.1

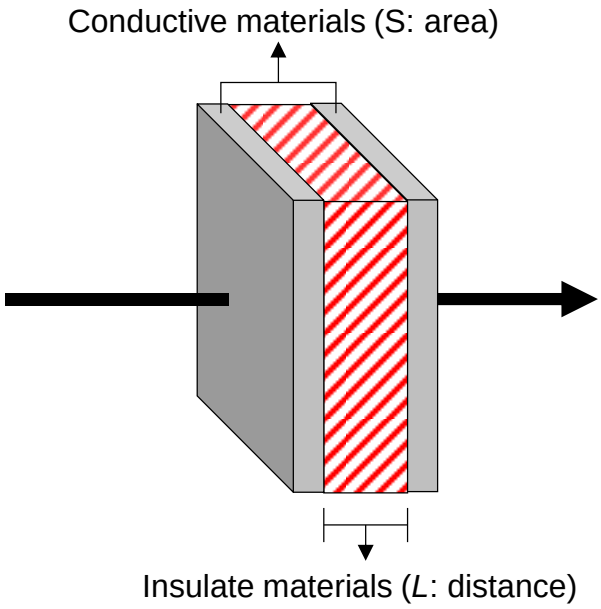

Figure 1.5.1. Principle of capacitor

$$C = \varepsilon_0 \varepsilon_s \frac{S}{L}$$

$$Q = C \times E$$

$$W = \frac{1}{2} C \times E^2$$

C: electrostatic capacity
ε_0: dielectric constant under vacuum
8.8554×10^{-12} (F / m)
ε_s: dielectric constant of the insulate material
S: effective electrode area (m^2)
L: distance between electrodes (m)
Q: electrification (C)
E: voltage (V)
W: energy (J)

Figure 1.5.2. Principle equations of electrostatic capacity

Capacitance (C) is the ability of a material to store an electrical energy. S is the area of conductive materials (electrodes) and *L* is the distance between electrodes. Their relations can introduce the dielectric constant (ε_s) of the insulate material (ε_0 is the dielectric constant under vacuum). From the capacitor principle, we can get that the one of the important factor is the thickness of insulate materials.

Recently, this capacitor expands their application for automobile are. Especially, the automobile will be developed to electrical automobile in the future. High performance capacitor is highly desired. Figure 1.5.3 shows the capacitor classification.

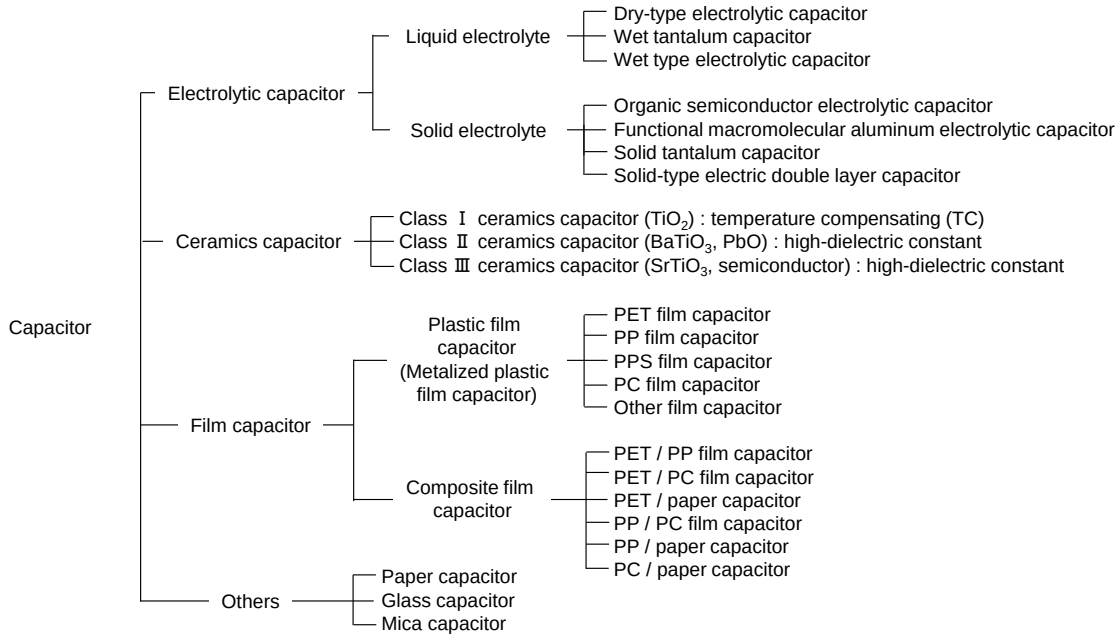

Figure 1.5.3. Classification of capacitor [Rubycon Corporation]

Film application will develop capacitor's full potential. When deposit layer upon layer of capacitor, their performance will be improved to according to increasing number of layers and also miniaturization of capacitors is one of important factor to improve their ability. Why film capacitor is desirable materials comes from their process ability. Polymer processing had plastic capacitors developed in this field.

1.5.2. Polypropylene Film for Capacitor

PP is the most desirable material in plastic film capacitors because of its balanced ability. The important factors for capacitor film are mentioned in Table 1.5.1. Mainly 4 kinds of polymer have been applied for capacitor. In industrial field, this capacitor has been mainly developed in automobile fields. And this field will develop as electrical automobiles in the future.

Its desirable ability for PP is mainly the thickness and long-term stability. Developments of processing ability have been contributed the preparation of polymer thin film for capacitor application. According to industry, the thickness of PP film became almost less than 3 μm in these last few years as I mentioned in Table 1.5.1. When we make PP film thinner, it is harder to prepare without clarify the structure property relationship. And also the long-term stabilization of PP film is necessary for understanding of its performance and structure relationship.

Recently, some researchers found that the relationship between crystalline diameter of PP and its property of electrical breakdown voltage (BDV). In this finding, it was clarified the smaller diameter of crystalline gives stronger BDV properties. As mentioned in Figure 4.1. This finding indicates the importance of morphology control of PP materials.

Improvement of BDV properties for capacitor application of PP was aimed in this chapter. In addition, a molecular mass dependence of crystallization in PP is not yet well established. Therefore, crystalline structure was characterized by using various molecular weight of PP firstly.

Table 1.5.1

Characteristics of plastic films for capacitor application [Rubycon corporation]

Characteristic	PP	PET	PPS*[1]	PEN*[2]
Thickness (μm)	3.0 – 25	1.0 – 25	1.5 – 25	1.0 – 25
Maximum working temperature (˚C)	80 – 105	120 – 130	130 – 140	120 – 140
Dielectric constant (1kHz at 20˚C)	2.2	3.2	3.0	2.9
Dielectric loss tangent (1kHz at 20˚C)	0.0002	0.003	0.0006	0.004
Volume resistivity (Ωcm)	$> 10^{17}$	$> 10^{18}$	$> 10^{17}$	$> 10^{17}$
Water absorption (% at 75 % humidity)	< 0.01	0.4	0.05	0.3
Glass transition temperature (˚C)	0	69	92	121
Breakdown voltage (kV / mm)	200 - 400	120 - 280	180	300

*[1]Polyphenylenesulfide

*[2]Polyethylene naphthalate

1.6. Objective

The objective of this research is to improve the life-time of PP materials by encapsulation and morphology control. Chapter 2 shows the G4-HBP effectiveness in PP matrix and discussion of its stabilization mechanism. Chapter 3 shows the generation effect for stabilization and applicant for PP nanocomposites. Chapter 4 shows the preparation of dendritic polymer on filler surface to elongate the life time of PP nanocomposites. Chapter 5 shows the improvements and prediction of PP film durability for long term capacitor application.

Chapter 2

Long-term Stability of Polypropylene materials by Hyperbranched Polymer

2.1. Introduction

As already mentioned, PP is one of the most widely used polyolefin because of its low cost, good processability, high chemical resistance, light weight, high melting point and well-balanced mechanical properties. In addition, because of the wide application and low environmental impact, further development of PP materials has been desired.

Basically, PP is easy to degradate due to heat and light originally, and the addition of various antioxidants is essential in order to obtain practical stability because PP has tertiary hydrogen which is easy to generate radicals compared with other carbons. Although there have been researched for the development of various antioxidants, there are still remain a matter of research. When considering the long-term usage of PP, not only the efficiency of the antioxidants but also the reduction of the physical loss of antioxidants, such as volatilization and leaching from PP matrix is important. One of the main approaches to solve these problems is the usage of high molecular weight antioxidants. However, because high molecular weight antioxidants decrease the mobility of themselves in the matrix at the same time, the combination with low molecular weight antioxidant is necessary.

Specific structure of HBP, which has a lot of branched chain, shows unique properties. Generally, linear polymer is easy to entangle each other but HBP has no entanglement because of the structure [55]. When their molecular weight is almost same, difference of their viscosity arises from a difference in their nature. Linear polymer shows higher viscosity with increasing its molecular weight however HBP is opposite. Dendrimer is one kind of branched polymers which can be synthesized by a precision synthesis. On the other hand, HBPs can be produced by one-pot synthesize,

which deliver promising results for industrial applications [56]. They are also called "dendritic polymer". There is density difference, which has its roots in functional groups, between its inside and outside in dendritic polymer like these. These functions can be applied as drag delivery carriers because they can capsule other materials with molecular size [57]. In medical field, the application of dendritic polymers already has been started. By changing the point of view, it is possible for PP to apply dendritic polymer as carriers for functional molecules like antioxidants. This strategy suggests that the HBPs might not only prevent the volatilization of antioxidants and also keep their diffusion in PP matrix by acting as molecular carrier. Bergenudd et all. suggested that the immobilization of antioxidants on HBP was useful to elongate polymer life-time in previous report [58]. However, this strategy is still in faithful accordance with traditional method.

The purpose of this chapter is to elongate the life-time of PP materials by the addition of HBP. It is highly possible that this strategy improves the efficiency of antioxidants as a molecular carrier. As already mentioned, two important factors for PP stabilization have been considered "Suppressions of antioxidants volatilization" and "Keeping diffusion of antioxidants". This strategy can achieve the development of highly stabilized PP materials.

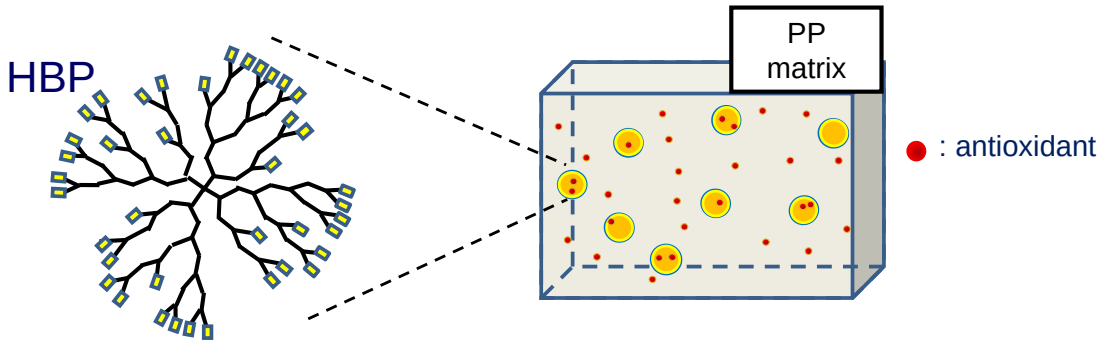

Figure 2.1 concept of this work

2.2. Experimental Section

Materials

Unstabilized PP powder polymerized by Ziegler-Natta catalyst was used as the matrix polymer (*mmmm* = 95 mol%, M_n = 57,000, M_w = 290,000, MWD = 5.02). *n*-octadecyl-3-(4'-hydroxy-3',5'-di-*t*-butylphenyl)propionate (ADEKASTAB AO-50) and butylated hydroxytoluene (BHT) was donated by ADEKA Co. Generation 4 hyperbranched polymer (G4-HBP, molecular weight = 7323 g/mol, 64 hydroxyl end groups) was purchased from Aldrich Chemical Company. SiO_2 nanoparticle (AEROSIL®90G, average diameter of 20nm, surface area of 90 m^2/g) donated by Nippon Aerosil Co., Ltd. was dried in vacuum for 6 hour at 180°C before melt mixing. Tetrahydrofuran (THF) without any antioxidants and *o*-dichlorobenzene (ODCB) purchased from Kanto Chemical Co., Inc. were used without further purification.

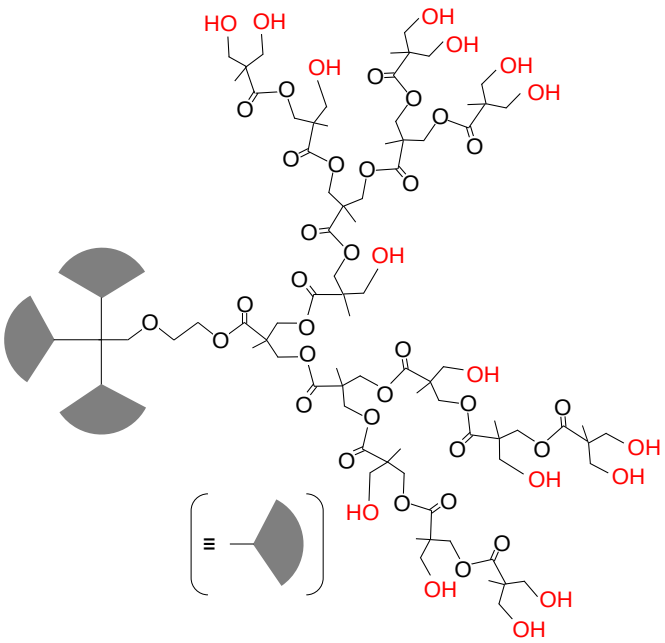

Figure 2. 2. Structure of the generation 4 hyperbranched polymer

On the other hand, the relationship between antioxidants and G4-HBP was also evaluated by using 7 kinds of antioxidants. They were donated ADEKA Co. and Toyotsu Chemical Co. Figure 2.3 and Table 2.1 shows their structure and information.

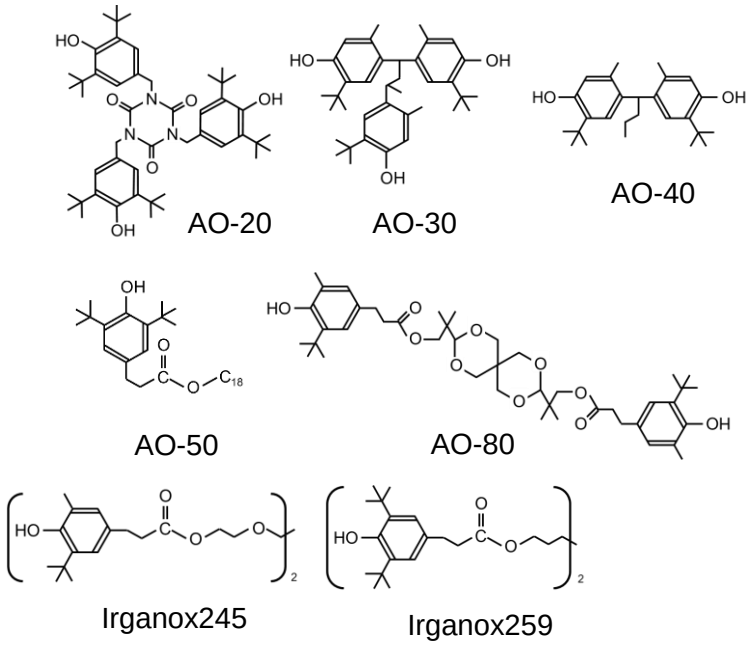

Figure 2.3 Chemical structure of antioxidants

Table.2.1 Antioxidants information

Product name	Molar weight (g/mol)	Melting point (˚C)
AO-20	784	220-222
AO-30	545	183-185
AO-40	383	210-214
AO-50	530	50-52
AO-80	740	110-120
Irganox245	586	76-79
Irganox259	638	180

Preparation

Blend Samples were prepared by melt mixing using two-roll (Imoto Machinery Co., Ltd.) mixer with a given amount of AO-50, and/or G4-HBP, respectively. The PP powder was blended in solid state with AO-50 at room temperature before melt mixing. The blended PP powder was kneaded by two-roll mixer at 185°C for 15 min to prepare a master batch contained 1.0 wt% of AO-50. And then a given amount of the master batch was added into the kneaded PP powder by blending on two-roll mixer at 185°C for 5 min. The mixture was kneaded for another 10 min with/without G4-HBP. The samples thus prepared were collected and subsequently stored in refrigerator. All the final products contain 0.07 wt% of antioxidants.

Film preparations were performed after melt-mixing. The melt-mixed sample was melted at 230°C for 5 min and then pressed at 10MPa for another 5 min. The pressed sample was immediately annealed at 100°C for 5 min, trying to keep constant crystallinity. Film thickness was kept constant (100 μm).

Characterizations

Differential scanning calorimetry (DSC) was performed using Mettler Toledo DSC 822. The measurement was carried out under a nitrogen atmosphere with heating and cooling rate of 10°C/min. Heating was started from below room temperature and rate of 10°C/min. Crystallinity was determined by taking the peak value of scans, respectively.

Tensile tests were carried out at room temperature using dumbbell-shaped

specimen at a crosshead speed of 1.0 mm/min. Tensile specimens were cut from the films and the testing was done with a Abecks DAT-100 at room temperature.

The oxidation induction time (OIT) measured by CLA strongly offers an indirect measure of life time of the sample films. Not only that, but these observations lead to the conclusion that the CL method can be used to screen the stabilizer effectiveness in PP. The chemiluminescence (CL) emission of PP films stabilized with antioxidants was studied at 150 or 180°C under dry air (100 ml/min) by Chemiluminescence analyzer (CLA, CLA-ID-HS, Tohoku Electronic Industrial Co. Ltd.). CL signal was counted for a period of 60s. Samples pieces were located on aluminum pans which were placed on the heating stage and adjusted to the required temperature.

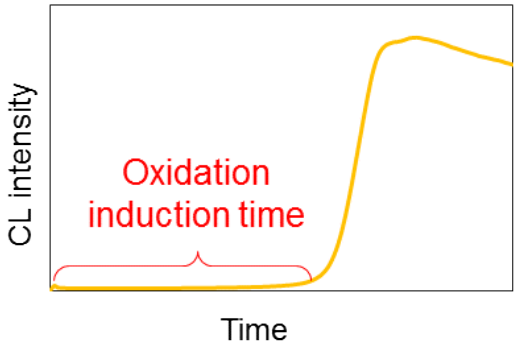

Figure 2.4. Typical CL spectra of stabilized PP

Volatilization tests were performed by Thermogravimetric (TG, Mettler Toledo TG50) analysis at 100°C under nitrogen atmosphere (50 ml/min). The data was collected on film samples contained 5.0 wt% of BHT.

Details of FT-IR emission measurements were shown in my minor research.

Table 2.2. Measurement conditions of FT-IR emission

Time (min)	180
Temperature (°C)	150
Flow rate (air, l/min)	12.0
Number of scans	256

2.3. Results and Discussion

Firstly, total results of this work were shown in Table 2.3.

Table 2.3

Sample information

	G4-HBP (wt%)	X_c (%)	Tensile strength (MPa)	Young's modulus (MPa)	Elongation at break (%)	OIT at 180˚C (h)	OIT at 150˚C (h)
PP	-	54.4	35.2	672	>300	0.4	21
PP/G4-HBP	1.0	52.7	35.0	670	>300	1.2	129

Table 2.3 shows the effects of G4-HBP added to PP. From this table, it was suggested that the addition of G4-HBP hardly affects to the crystallinity and the mechanical properties of PP materials, when it was 1.0 wt%.

According to these results, it was concluded that the other factors which related to PP morphology and its structure can be deleted. Therefore, we can focus on the

discussion about HBP effect.

CL analysis is also widely used for detect the initial stage of degradation with very high sensitivity. It is well known that degradation is accompanied by very weak emission. Figure 2.5 shows the results of CL measurements at 150˚C and 180˚C.

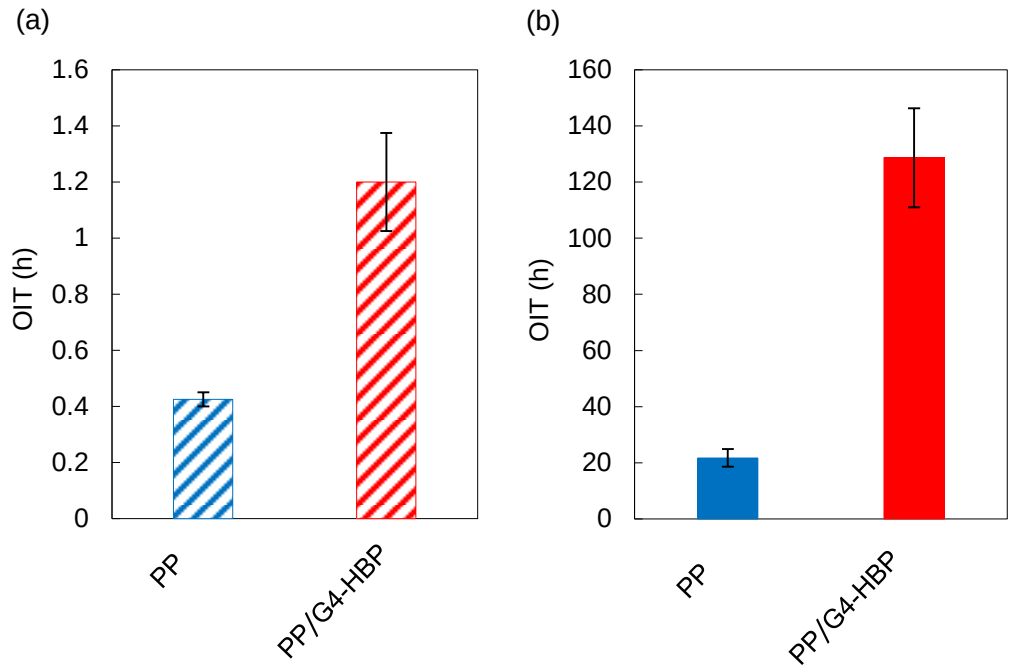

Figure 2.5. CL analysis of PP and PP/G4HBP in (a) molten state at 180˚C and (a) solid state at 150˚C

The addition of G4-HBP was re improvement of OIT on both measurements at 180˚C and 150˚C. On the measurement in molten state at 180˚C, PP/G4-HBP shows three times as long as PP. PP/G4-HBP at 150˚C elongates its OIT almost 6 times longer than PP. Great improvements of OIT were observed by adding G4-HBP. This suggests that the effect of G4-HBP in solid state much higher than that in molten state.

The reason why solid state shows higher improvement of OIT may be related to PP crystallinity. When PP was crystalized, the amorphous region, which is easy to degradate compared with crystal region, decreases in contrast of its crystallinity. Therefore, it is possible that there is an increase in the percentage of G4-HBP, which only can exist in amorphous region of PP. According to OIT measurements, these improvements might be come from the encapsulation of G4-HBP for antioxidants.

OIT measurements of PP and PP/G4-HBP after extraction of antioxidants by solvent were performed in order to confirm the effects of G4-HBP. AO-50 can dissolve in all proportions with hexane. Figure 2.6 shows the results of OIT measurements.

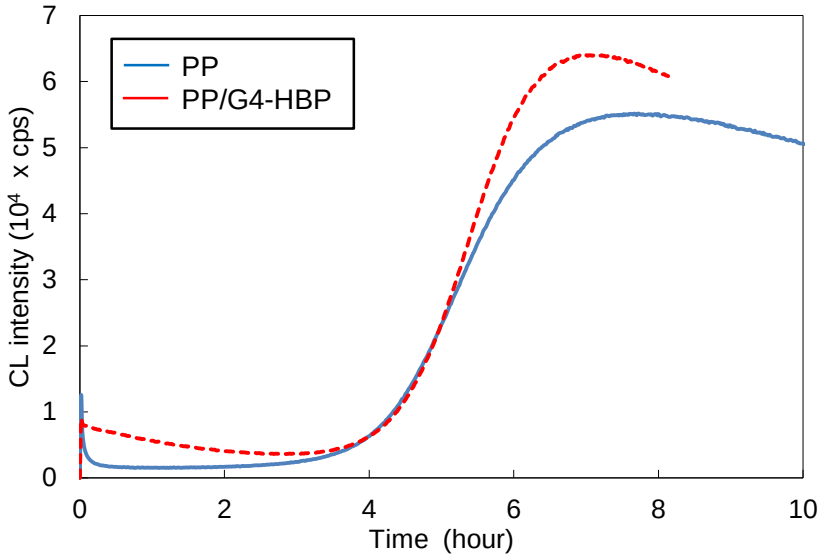

Figure 2.6. CL analysis of PP and PP/G4-HBP at 130˚C after extraction of AO-50 by hexane

Hexane was chosen as a solvent for antioxidants extraction because AO-50 can be

dissolved easily. CL analysis showed almost all same OIT between PP and PP/G4-HBP. This result indicates that the OIT improvement came from not G4-HBP itself but the supplement the efficiency of antioxidants by G4-HBP. It was also strongly suggested that the encapsulation of G4-HBP might be exist.

On the other hand, we must consider about grafting reaction between G4-HBP and antioxidant by dehydration reaction of hydroxyl groups. However, it was suggested that there are no grafting reaction between G4-HBP and antioxidants. Why there are no grafting reaction is that the CL results showed same time OIT both PP and PP/G4-HBP after antioxidants extraction.

The reason why the addition of G4-HBP improved the OIT of PP is still not unclear. Therefore, volatilization of antioxidants was characterized by TG analysis. Figure 2.7 shows the results of volatilization of PP/BHT and PP/G4-HBP/BHT.

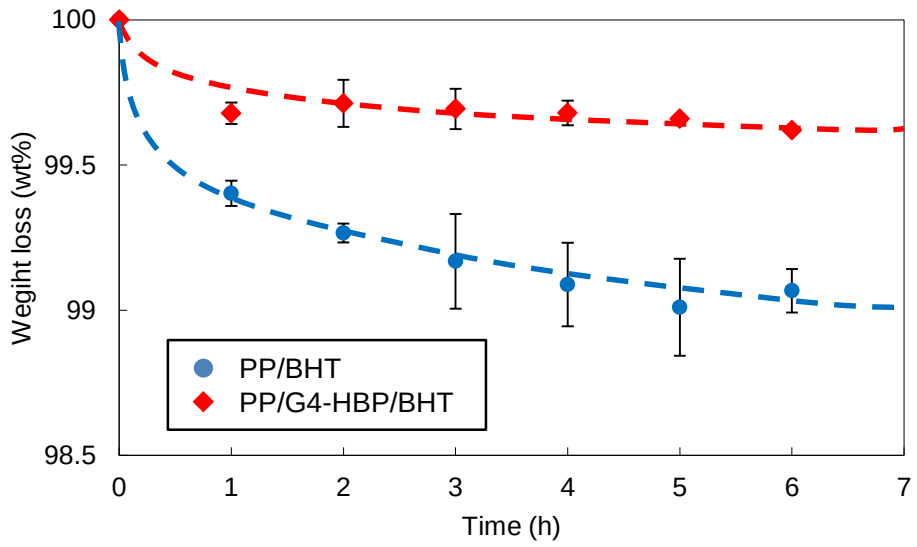

Figure 2.7. Effect of G4-HBP as a volatilization of BHT in PP matrix

BHT, which is the lowest molecular of antioxidants, was chosen in this work. PP/G4-HBP/BHT was decreased at low rate compared with PP/BHT. It suggests that G4-HBP in PP matrix suppresses the volatilization of BHT. However, suppression of AO-50 was not observed by TG analysis.

FT-IR emission was performed to clarify the reason why suppression of AO-50 was not observed. The principle of FT-IR emission was shown in Figure 2.5. FT-IR emission is different from these measurements. It is much useful for real time quantitative analysis of samples. In the case of FT-IR emission, samples are needed in order to get infrared spectrum. The heated infrared spectrum corresponds to absorption spectrum. Thin films which are less than 2 μm are necessary for emission measurements.

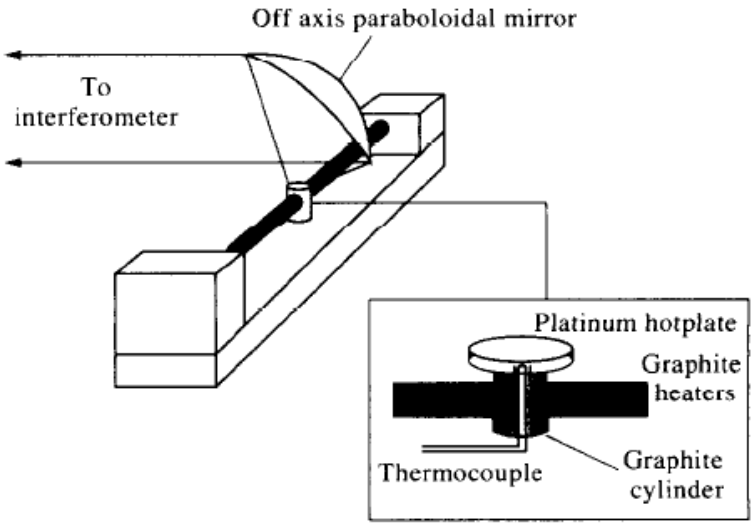

Figure 2.8. Schematic diagram of the emission cell used with the FT-IR spectrometer [59]

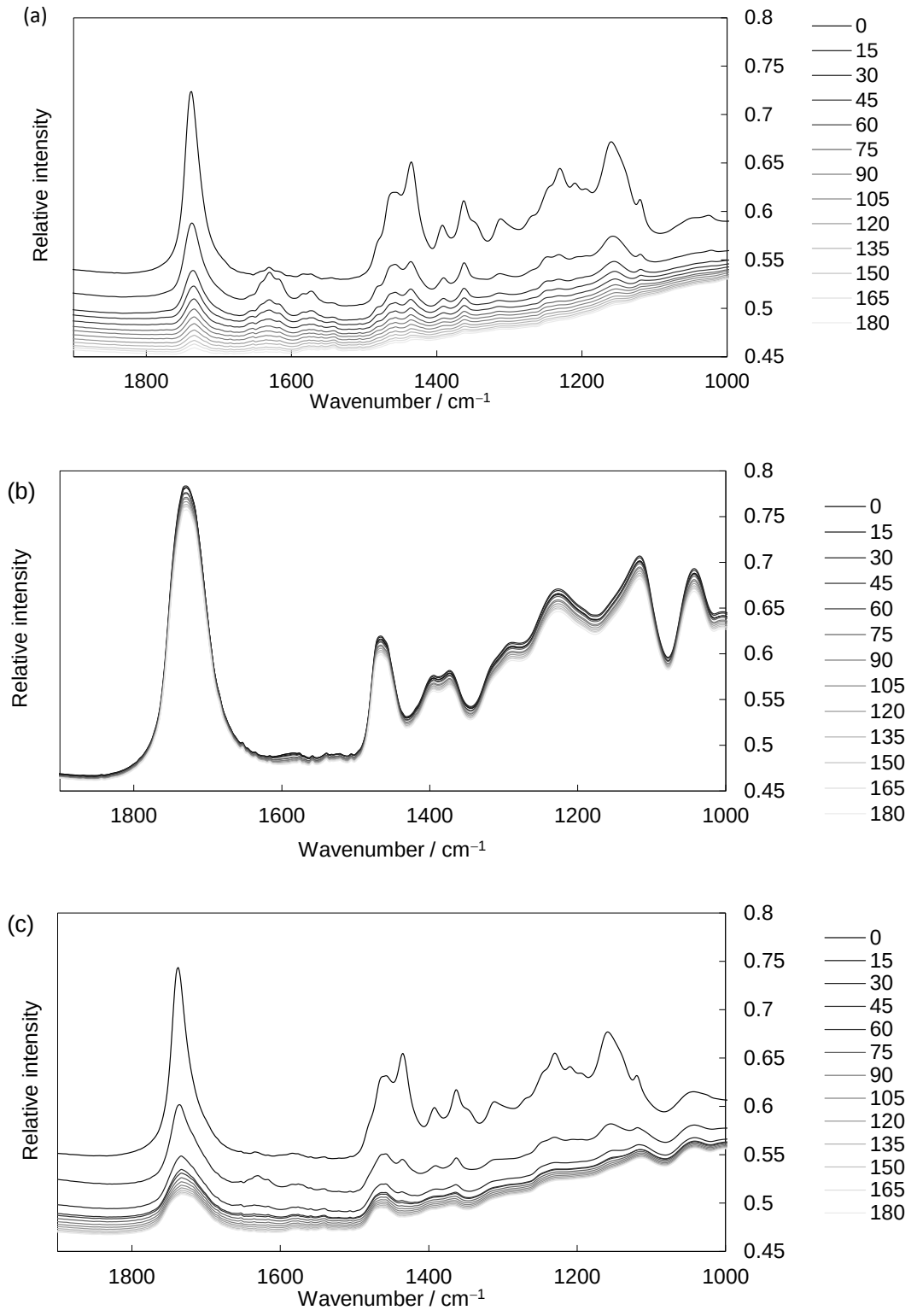

Figure 2.9. FT-IR emission analysis (a) AO-50, (b)G4-HBP, (c) mixture of AO-50 and G4-HBP.

Figure 2.9 shows the results of FT-IR emission. These results suggest that the AO-50 degrease its spectra with increasing measurement time (Figure 2.6 (a)). On the other hand, G4-HBP has remained its intensity of high during the measurement (Figure 2.6 (b)). The spectra of mixture of AO-50 and G4-HBP behaved like AO-50 (Figure 2.6 (c)). From these results, it was confirmed that the G4-HBP had no spectra change during the measurement. Therefore the G4-HBP contained mixture was also changed nothing. The peak intensity of AO-50 (a) is getting degrease with increasing the measurement time and it suggests the volatilization of AO-50.

However, it is difficult to discuss the comparison of samples because of their low data. It is necessary for characterization of G4-HBP effect to subtract itself as a background. Figure 2.10 shows the spectra of FT-IR emission after subtraction of spectra at 180 min as a background. And then we can discuss about the interaction between AO-50 and G4-HBP.

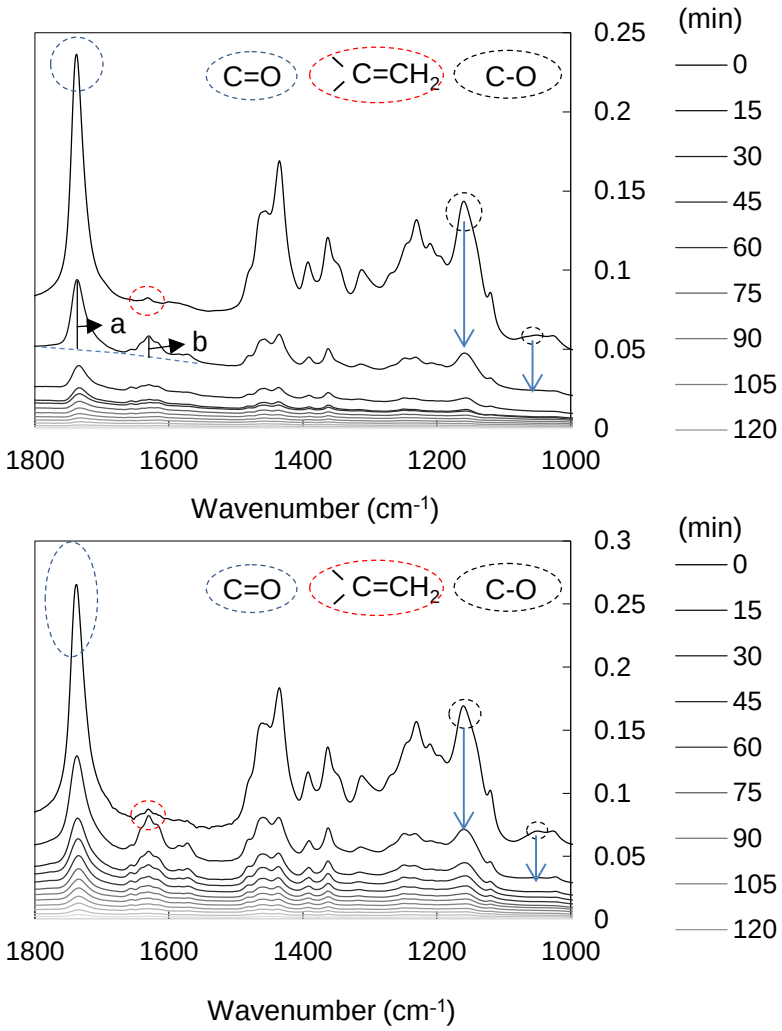

Figure 2.10. FT-IR emission spectra of (upper) AO-50 after subtraction of AO-50 spectra at 180 min as a background (under) mixture of AO-50 and G4-HBP after subtraction of the mixture at 180 min as a background

The change of time dependence of spectra was clearly observed from Figure 2.7. Especially, the intensity at 1630 cm^{-1} became stronger and stronger with time. This intensity suggested that the structure change of AO-50 and the number of carbon double bonds was increased during the measurements.

Pospisil et al. reported the structure change of Irganox 1076 which is same chemical structure with AO-50[60]. Their report showed that the main products after the reaction of antioxidants were dimers. Otherwise, the structure which was shown in Figure 2.11 also can be generated on thermal degradation as a final product.

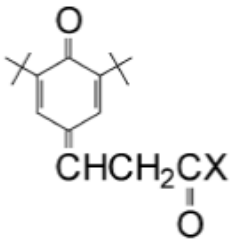

X = -O-$C_{18}H_{37}$

Figure 2.11. One of deactivated structure of AO-50

In this work, it may be possible to generate like a structure shown in Figure 2.8. And also the peak intensity at 1050 and 1240 cm^{-1} origin form ester bonds of AO-50 is also getting weaker with increase measurement time. It is highly possible that the decomposition of ester bonds occur during the measurement (Figure 2.8: point X). In addition, the intensity at 1740 cm^{-1} origin from ester bonds (carbon oxygen double bonds) still remains, which assumes the existence of AO-50, when comparing with that at 1050 and 1240 cm^{-1}. On the other words, the reason why the whole intensity decreased with increasing the time is that both volatilization and decomposition of AO-50 are occurred during thermal aging.

More discussions are necessary for clarification of the mechanism of HBP stabilization. The intensity at 1740 cm^{-1} and 1630 cm^{-1} was defined as a standard peak (a) and decomposition peak (b), respectively. Standard peak means the remaining AO-50 without any structural change and decomposition peak means the decomposition of AO-50. When we want to discuss the interaction, it is useful to estimate the ratio between remaining and decomposition. Figure 2.12 shows the deactivation rate by dividing the (b) and (a) with measurement time.

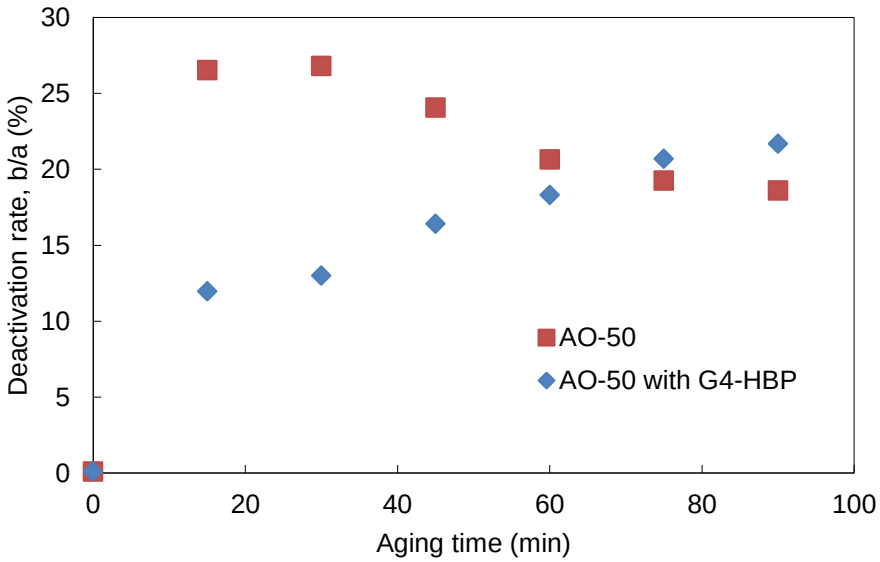

Figure 2.12. Deactivation rate (b/a) of AO-50 with/without G4-HBP

Compared with AO-50 only, deactivation rate of AO-50 was decreased by coexisting with G4-HBP in early stage of the measurements (0 – 60 min). It suggests that the G4-HBP can suppress the deactivation of antioxidants in early stage. It is well known that the preventing the early stage degradation is more important for long term usage of materials because degradation is expanded exponentially. Therefore, it is

highly possible that the G4-HBP prevents deactivation of antioxidant and then elongates the lifetime of PP materials.

This deactivation mechanism might be related to hydrogen bonds between G4-HBP and antioxidants. Both G4-HBP and AO-50 have hydroxyl groups and ester bond witch can form hydrogen bonds.

It might be related to antioxidants volatilization because coexisting with G4-HBP suppresses the early stage decomposition of antioxidant. One possibility is that G4-HBP can suppress low molecular antioxidants, which can be generated after decomposition of antioxidants. This explanation is reasonable for the understanding of stabilization mechanism.

Structure-performance relationship between antioxidants and G4-HBP were very important for understanding its stabilization mechanism.

Figure 2.13 shows the stabilization effect of G4-HBP by changing the antioxidants. OIT results from CL analysis showed all the antioxidants were affected by G4-HBP.

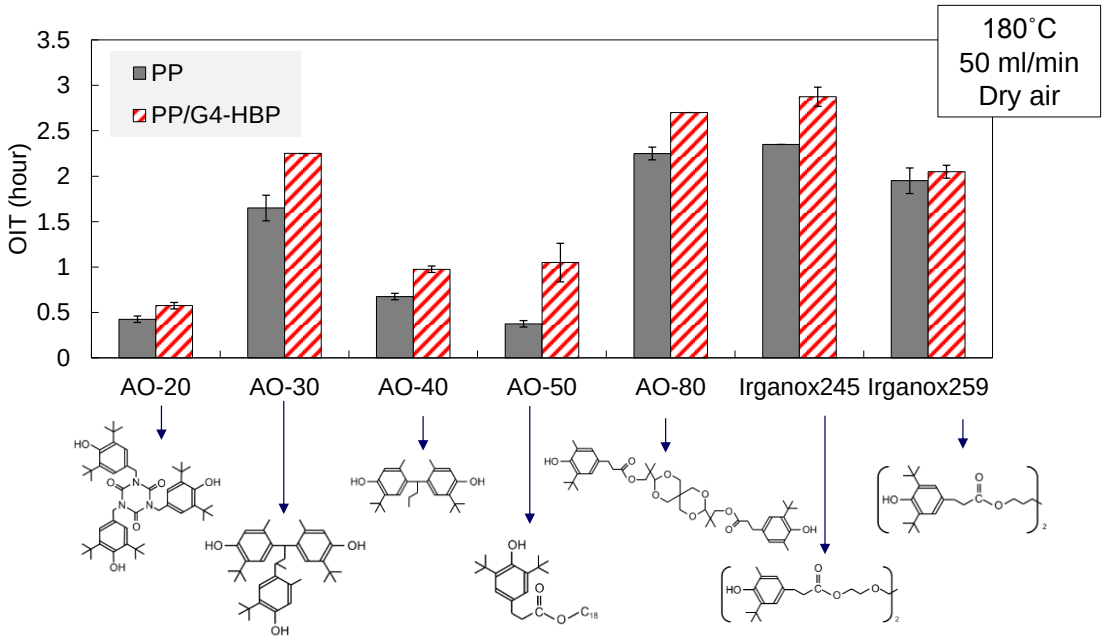

Figure 2.13 CLA analysis by using 7 kinds of antioxidants.

All the stabilizers showed the elongation of OIT by adding G4-HBP. However, the relationship between antioxidants structure and OIT improvements is difficult to clarify from Figure 2.13. Molecular weight of antioxidants is one of the important factors to define antioxidants characteristics. Therefore, the summary of molecular weight and OIT improvements were shown in Figure 2.14

Following equation was used for characterization of OIT improvement by G4-HBP.

$$\Delta OIT = (OIT \text{ of } PP/G4\text{-}HBP) - (OIT \text{ of } PP)$$

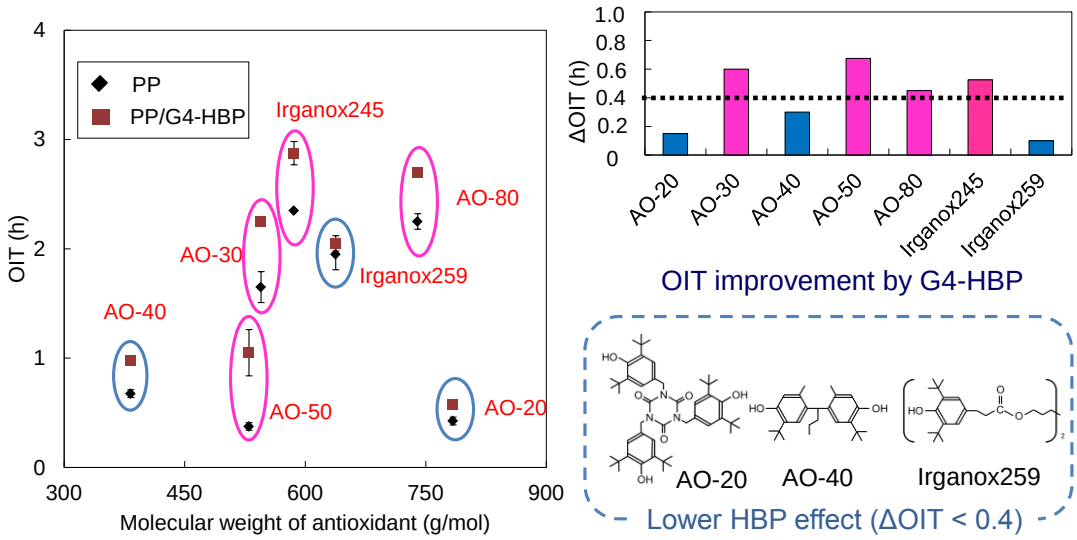

Figure 2.14 Summary of relationship between molecular weight and OIT improvements

It was defined that lower stabilization effect by G4-HBP was the improvement of 0.4 or less in Figure 2.14. However, the relationship between chemical structure and *Δ*OIT was still unclear.

Figure 2.15 was focused on melting point of antioxidants.

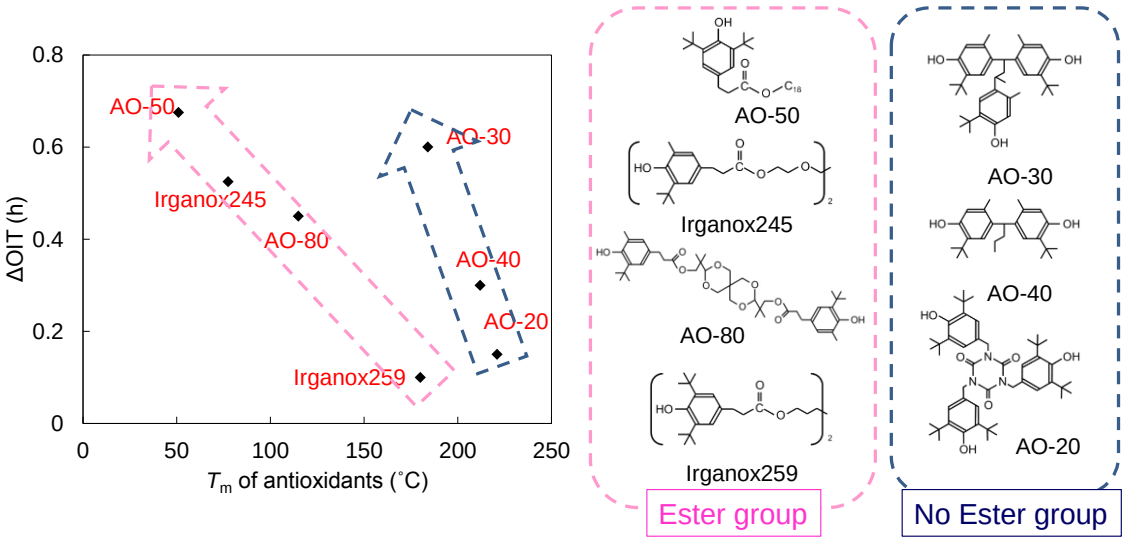

Figure 2.15 Relationship between the OIT improvements and melting point of antioxidants.

This result suggested that the antioxidants structure performance for OIT improvement by G4-HBP. It was confirmed that the stability (OIT) of PP was depends on the melting points of antioxidants. In addition, the presence or absence of ester bonds in antioxidants might be the key to decide the stabilization mechanisms by HBP.

2.4. Conclusion

In this chapter, The G4-HBP effects for the stabilization of PP materials were researched and discussed. The highly stabilized PP material was prepared by addition of G4-HBP. It was confirmed that the G4-HBP has no stabilization ability itself and the volatilization of antioxidants from PP matrix was suppressed by G4-HBP. These results suggest that the G4-HBP play as a molecular encapsulation. And also the antioxidants structure might be affect to OIT improvement. Especially, the presence of ester bond in antioxidants might be the key for this stabilization.

Chapter 3

Generation Effect of Hyperbranched Polymer and Preparation of Highly Stabilized Polypropylene Nanocomposites

3.1. Introduction

PP is one of the most widely used polyolefin because of low cost, good processability, high chemical resistance, light weight, high melting point and well-balanced mechanical properties. Because of its wide application and low environmental impact, further developments of PP materials have been eagerly desired. Nanocomposites will expand the application area of PP materials because of their great improvement of mechanical properties at low filler levels. This improvement is a consequence of the extremely high interfacial area and short distance between filler particles. However, the addition of fillers deteriorates thermal and photo stability of PP. This is one of the reasons why the application of PP nanocomposites has not been expanded as expected [61-64].

PP easily degrades by heat and/or light as I already mentioned. The addition of various stabilizers is essential to obtain practical stability. For the long-term use of PP, not only the efficiency of the stabilizers but also the reduction of the physical loss of stabilizers by volatilization and leaching from PP matrix is important [65,66]. In addition, PP composites promote the physical loss of stabilizers from the filler/matrix interface because of poor adhesions [43]. Therefore, the inhibition of physical loss of stabilizers is particularly important for the stabilization of PP nanocomposites. One of the main approaches to inhibit the physical loss of stabilizers is the usage of high molecular-weight stabilizers, which have low mobility [67].

Our group has found the stability of PP was greatly improved by the addition of HBP, which is one of well-known dendritic polymers. Though HBP could not stabilize PP as itself, it significantly reduced the physical loss of stabilizers without

compromising the mobility of stabilizers. The merit of this method was to improve the efficacy of conventional stabilizers without developing new stabilizers. The same technique was successfully applied in this study to significantly elongate the lifetime of PP nanocomposites. We found synergetic stabilization using nano SiO_2 mixed with PP.

Nanocomposites are expected to expand the application area of PP materials. High interfacial surface area of filler/matrix can be achieved by adding a few wt% of nano filler compared with conventional micro filler. Furthermore, nanocomposites has been expected the filler/filler interaction for reinforcement of the mechanical properties. It can also significantly improve the transparency and gas barrier. However, because of the poor dispersion of nano fillers in PP matrix, the mechanical properties did not be improved as expected. The long-term usage of PP nanocomposites is also the problems because of low light stability and low thermal stability. This is the reason why application of PP nanocomposites has not been expanded as expected [41].

In addition, PP composite promotes volatilization of the antioxidant from the filler/matrix interface because of less interface adhesions [61]. Therefore, the solution of the problems for the volatilization and leaching of antioxidant is particularly important for PP nanocomposites.

3.2. Experimental Section

Materials

PP powder (*mmmm* = 95 mol%) was synthesized by bulk polymerization using a Ziegler-Natta catalyst. N-octadecyl-3-(4’-hydroxy-3’,5’-di-t-butylphenyl)propionate (ADK STAB AO-50) was donated as a hindered phenol stabilizer from ADEKA Co., Ltd. Spherical SiO_2 with an average diameter of 20 nm (AEROSIL®90G, Nippon Aerosil Co., Ltd.) was dried for 6 h at 180°C in vacuo. Hyperbranched bis-MPA polyester-16-hydroxyl, generation 2 (G2-HBP, M_w = 1750) and hyperbranched bis-MPA polyester-64-hydroxyl, generation 4 (G4-HBP, M_w = 7323) were purchased form Aldrich Co., Ltd. And used without further purification.

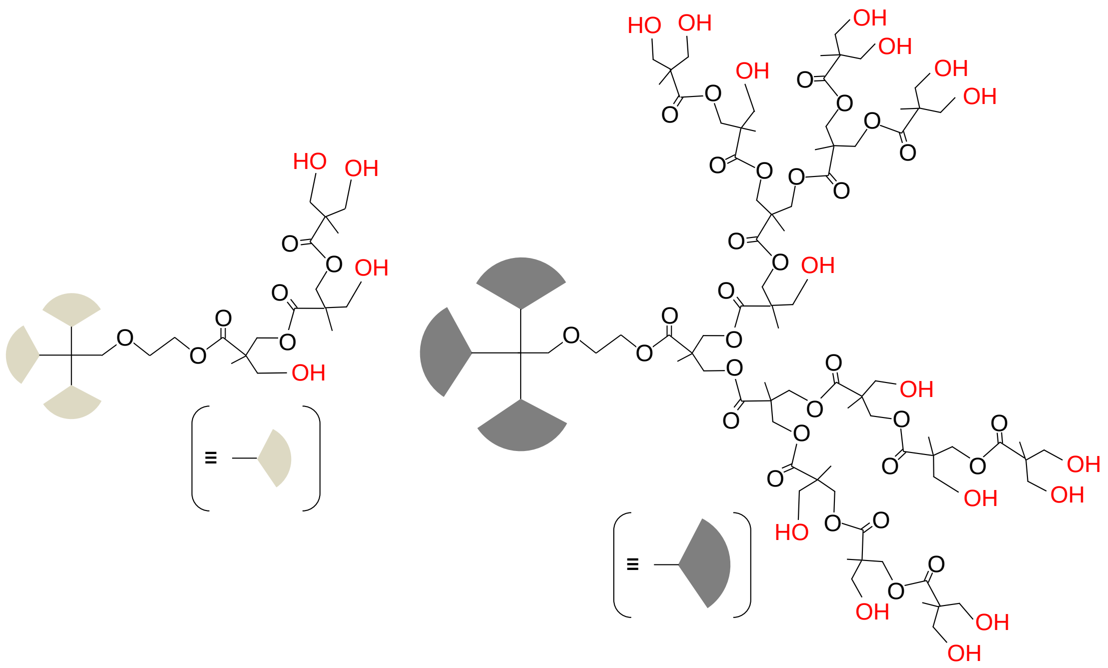

Figure 3.1 Chemical structure of (left) G2- and (right) G4-HBP

Sample preparation

PP powder and 0.07 wt% of AO-50 were melt-mixed using two-roll mixer at 185°C and 20 rpm for 15 min with 1.0 wt% of HBP and/or 5.0 wt% of SiO_2. Sample films were prepared by hot press at 230°C and 10 MPa with the thickness of 100 μm. The films were then quenched at 100°C for 5 min, followed by quenching at 0°C. The sample films were named as PP, PP/SiO_2, PP/G2-HBP, PP/G4-HBP and PP/SiO_2/G4-HBP. Sample components were shown in Table 3.1.

Table 3.1

Sample components

Sample	SiO_2 (wt%)	G2-HBP (wt%)	G4-HBP (wt%)
PP	-	-	-
PP/SiO_2	5.0	-	-
PP/G2-HBP	-	1.0	-
PP/G4-HBP	-	-	1.0
PP/SiO_2/G4-HBP	5.0	-	1.0

Characterizations

The crystallinity of sample films was determined by differential scanning calorimetry (DSC, DSC822, METTLER Co., Ltd). The sample was heated up to 200°C at a rate of 10°C/min. Tensile tests (DAT100, ABECKS Inc.) were carried out at room temperature using dumbbell-shaped specimen at a crosshead speed of 1.0 mm/min.

An accelerated degradation tests at 150°C under dry air (100 ml/min) were performed by a chemiluminescence analyzer (CLA, Tohoku Electronic Industrial Co., Ltd., CLA-ID2-HS). The thermal stability of samples was evaluated in terms of OIT.

The dispersion of HBP in the matrix was observed using scanning electron microscopy (SEM, HITACHI, S-4100) of fracture surfaces, where HBP was preliminary extracted by tetrahydrofuran. A fracture surface of the blended PP was obtained by freezing the sample in liquid nitrogen for 3 min and then breaking by bending. The fractured chunk was placed in solvent to extract the dispersed phase droplets, leaving holes in the matrix. The solvents used were THF to dissolve HBP droplets by sonication for 4 hour. All samples were sputter-coated with platinum-palladium. And then, the dispersed phase of G2-HBP or G4-HBP was observed from their fractal surfaces by SEM.

The dispersion of SiO_2 was characterized by transmission electron microscopy (TEM, Hitachi, H-7100). TEM images to observe SiO_2 dispersions were obtained from PP nanocomposites. All the samples were ultramicrotomed with a diamond knife (Diatome, Nisshin EM Co,.) on microtome (Leica, ULTRACUTS FCS) at −50°C to give sections with a thickness of 100 nm. The sections were transferred from ethanol

to Cu grids of 300 mesh.

Thermogravimetric analysis was performed by TG under air (50 ml/min) in a temperature range from 200 to 650 °C at a heating rate of 10°C/min to confirm a grafting amount of HBP on SiO_2. Ungrafted HBP was completely removed by repetitive hot filtration with ODCB at 140°C.

3.3. Results and Discussion

Table 1 shows the crystallinity and the mechanical properties of prepared samples.

Table 3.2

Sample information

Sample	OIT at 180˚C (h)	OIT at 150˚C (h)	X_c (%)	Tensile strength (MPa)	Young's modulus (MPa)	Elongation at break (%)
PP	0.4	21	54.4	35.2	672	>300
PP/SiO_2	0.6	18	51.5	37.4	790	133
PP/G2-HBP	0.8	65	52.3	35.8	672	>300
PP/G4-HBP	1.2	129	52.7	35.0	670	>300
PP/SiO_2/G4-HBP	1.3	190	51.7	35.9	766	140

The addition of SiO_2 improved the Young's modulus by 17.5%, while the addition of HBP hardly affected the mechanical properties of PP and PP/SiO_2. Also crystallinity of PP was hardly affected by adding HBP. From these results, we can focus on the discussions related to HBP stabilization without considering PP morphology effects.

Figure 3.2 shows OIT result at 180˚C and at 150˚C.

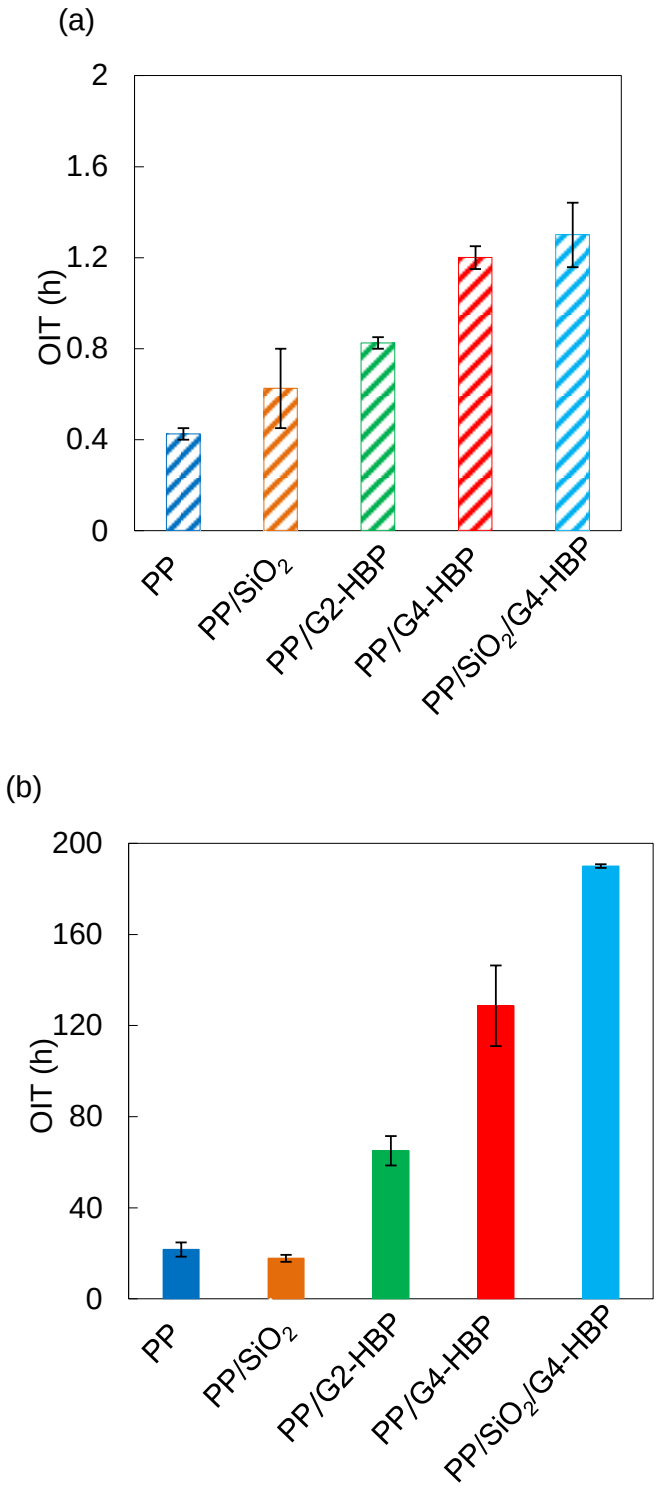

Figure 3.2. CL profiles of PP materials in molten state at 180°C (a) and solid state at 150°C (b).

Then, the effects of HBP on the stabilization of PP and PP nanocomposites were investigated. Figure 3.2 summarizes the OIT values of the samples at 150°C. The order of the stability was PP/SiO_2/G4-HBP ＞ PP/G4-HBP ＞ PP/G2-HBP ＞ PP ＞ PP/SiO_2. The addition of HBP to PP significantly enlarged the OIT value as compared with that of pristine PP.

The stabilization degree was sensitive to the generation of HBP that is G4-HBP showed almost the double improvement over G2-HBP. In contrast to the lower stability for PP/SiO_2 than for pristine PP, PP/SiO_2/G4-HBP showed the best stability among all. The addition of G4-HBP in the presence of SiO_2 elongated the OIT value more than that in the absence of SiO_2. Thus, we found that the addition of HBP was effective for PP nanocomposites, and that the synergetic stabilization appeared for PP/SiO_2/HBP.

Before discuss the mechanism about synergistic stabilization, we confirmed the stabilization ability of HBP itself. The result was shown in Figure 3.3.

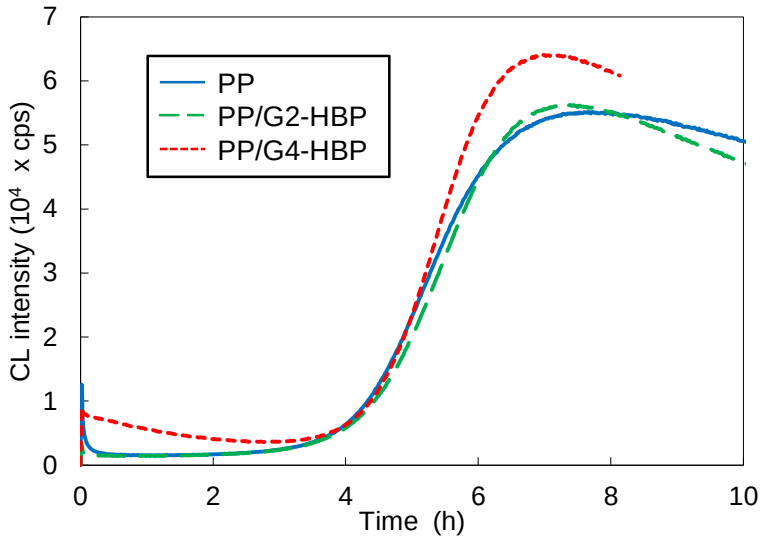

Figure 3.3　CL profiles of PP materials after extraction of AO-50 at 135˚C

After HBP extraction, PP, PP/G2-HBP and PP/G4-HBP showed same OIT. This result suggested that the HBP itself never prevent PP degradation same as chapter 2. Therefore, it is highly possible that G4-HBP can improve antioxidants efficiency in PP matrix by its functionality like encapsulation. Then, we need to discuss about the difference of G2- and G4-HBP. This generation differences strongly might affect to OIT improvement.

Figure 3.4 shows the dispersion of HBP in PP matrix.

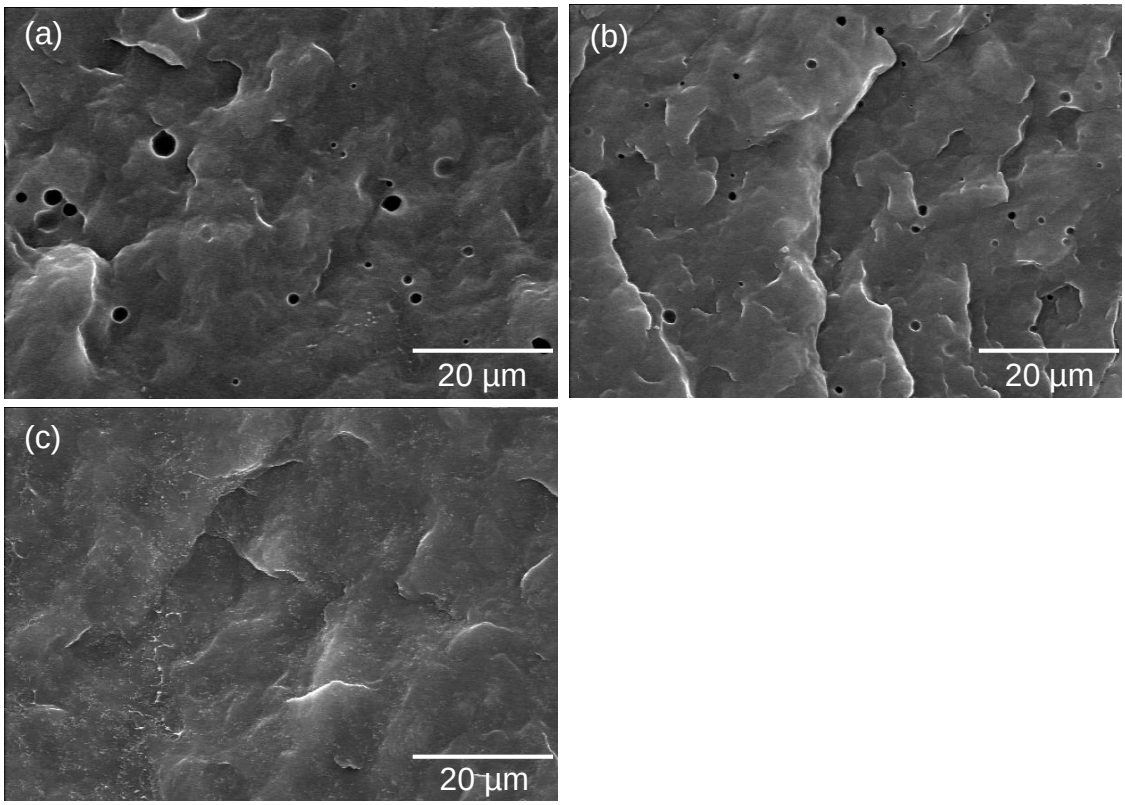

Figure 3.4.　SEM images of (a)PP/G2-HBP, (b)PP/G4-HBP and (c)PP/SiO_2/G4-HBP

Figure 3.4 shows the dispersion of HBP obtained by SEM observations for fracture surfaces, where holes correspond to the droplets of HBP in the matrix. The dispersion of G4-HBP in the matrix was better than that of G2-HBP, which might be correlated with the better performance of G4-HBP in stabilizing PP. Furthermore, no holes were observed for PP/SiO_2/G4-HBP, which suggested the possibility that HBP was in-situ grafted onto SiO_2 during melt mixing.

Next, Figure 3.5 shows the dispersion of SiO_2 in PP matrix.

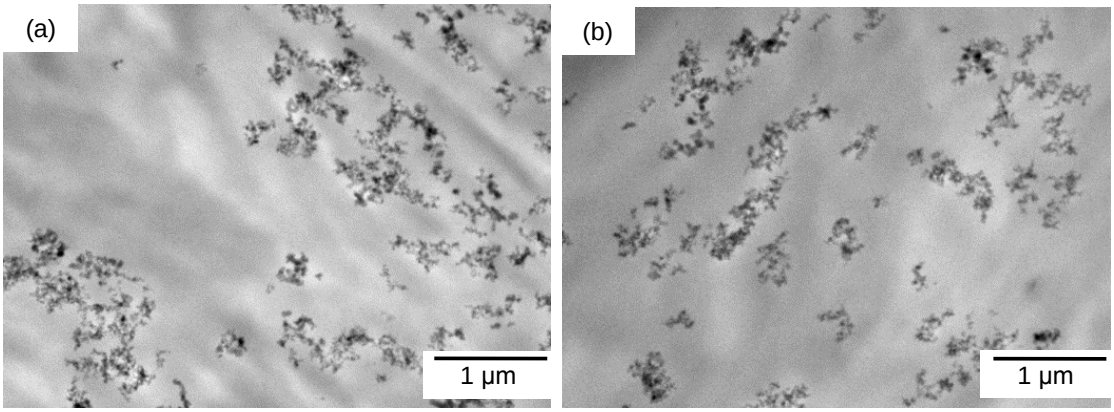

Figure 3.5. TEM images of (a)PP/SiO_2, (b)PP/SiO_2/G4-HBP

HBP has been known as a compatibilizer was expected to improve the dispersion of SiO_2 in the matrix. However, the dispersion of SiO_2 was hardly affected by HBP shown in Figure3.5.

As an additional experiment, TG analysis was performed under air in a temperature range from 200 to 650 °C to confirm a grafting amount of HBP on SiO_2. Ungrafted HBP was completely removed by repetitive hot filtration with ODCB at 140°C. The results were shown in Figure 3.6.

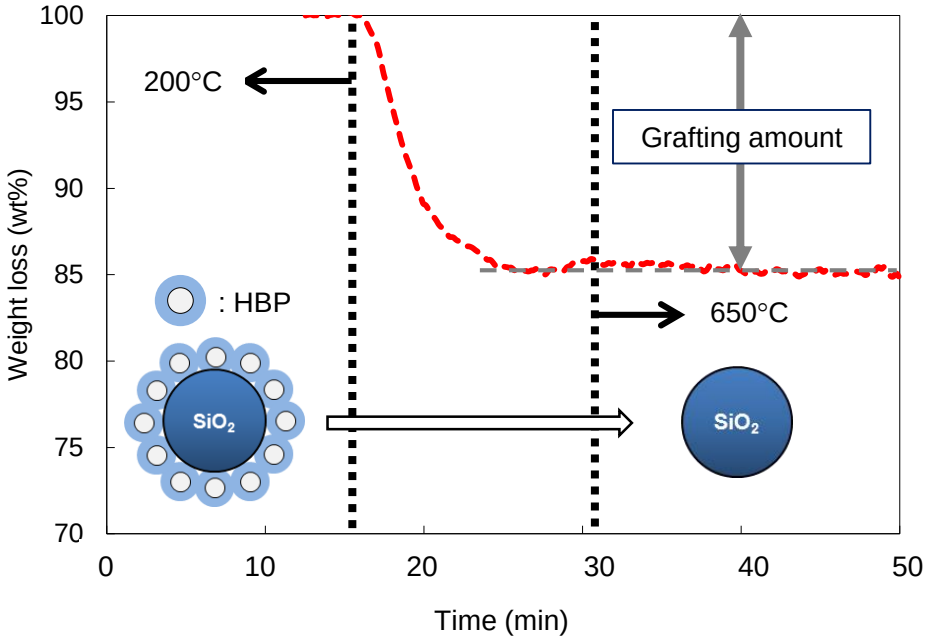

Figure 3.6. TG analysis of HBP grafting reaction on SiO_2 surface during melt-mixing

If grafting reaction of G4-HBP and SiO_2 was occurred during melt mixing, organic compounds must be remained on SiO_2 surface. It was confirmed that 14.0 wt% of organic compounds remained on SiO_2 surface. We estimated the reaction efficacy of G4-HBP. 99 % of used G4-HBP was reacted with SiO_2. This means almost all the used G4-HBP was reacted during melt-mixing. It looks too high as reacted amounts. However one G4-HBP molecule has 64 numbers of hydroxyl groups. That is to say, about 1.6 % of hydroxyl group is enough to achieve 99 % of this reaction. From these discussions, we can conclude that the G4-HBP was highly dispersed in PP matrix by

using SiO2 as a career and the function efficiency of G4-HBP was improved by this highly dispersion. This might be a reason why PP/SiO_2/G4-HBP was highly stabilized.

This additional experiment was conducted to confirm in-situ grafting of HBP onto SiO_2. It is believed as the origin of the synergetic stabilization when HBP and SiO_2 coexisted in PP.

After thermal filtration, functional groups in insoluble fraction were observed by FT-IR measurement. Figure 3.7 shows the results of FT-IR measurement.

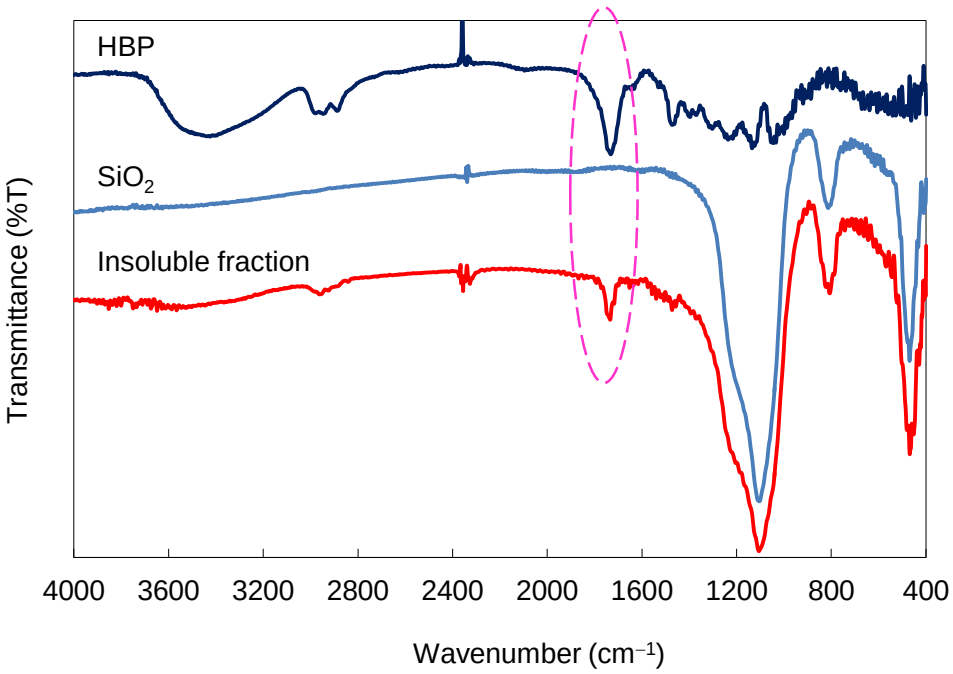

Figure 3.7 FT-IR spectra of HBP, SiO_2 and insoluble fraction

This result strongly proved that G4-HBP grafting reaction during melt-mixing because ester peak was observed in insoluble fraction.

3.4. Conclusion

A highly stable PP nanocomposite was prepared successfully by applying a new stabilization technology using HBP in this chapter. It was discovered that the addition of HBP is useful for the stabilization of not only PP but also PP nanocomposites. Especially, the stability of a PP/SiO_2 nanocomposite was significantly improved by a synergetic effect plausibly due to in-situ grafting of HBP to SiO_2 during melt-mixing.

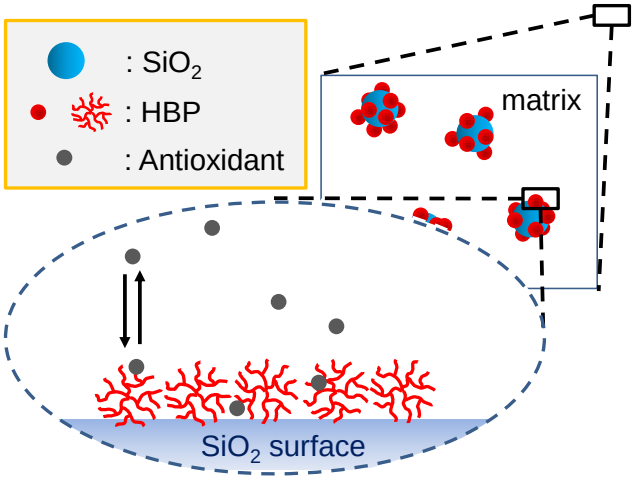

Figure 3.8 Concept of stabilization mechanism of PP/SiO_2/G4-HBP.

Chapter 4

Stabilization of Polypropylene Nanocomposites by Dendritic Polyglycidol Modified Nano-Filler

4.1. Introduction

Polypropylene (PP), as the most widely used thermoplastic, is featured with a large application area and a multitude of advantages such as good processability, high chemical resistance, light weight, low production cost, high melting temperature and good balance of mechanical properties. [68] The annual production of PP has reached 70 million tons all over the world, while the industrial attention has been paid on the development of value-added PP materials. Nanocomposites are one of the most promising strategies to the value addition: The inclusion of nano-sized filler can bring about great reinforcement as well as new functional properties which cannot be achieved using micro-sized filler [69,70]. Thus, PP-based nanocomposites have been a target of extensive researches, where the main concern has been to solve poor compatibility between chemically inert PP and inorganic filler. The addition of a compatibilizer and surface modification with short aliphatic chains have been studied in order to improve the dispersion and the adhesion of filler with PP.[4,5)]

In addition to mechanical and functional properties, the elongation of lifetime is practically required for PP-based nanocomposites: The inclusion of nano-sized filler often accelerates the oxidative degradation of PP [71-75]. Mailhot et al. studied the mechanism of enhanced degradation of PP/montmorillonite nanocomposites under UV light [75]. They claimed that a stabilizer might be concentrated around hydrophilic filler, thus reducing the efficiency of the stabilizer. It was also proposed that montmorillonite, an alkylammonium modifier and a maleic anhydride-grafted PP compatibilizer might generate photo-responsive species and/or catalyze the photo-oxidation of PP [76]. Iron impurities contained in clay also result in dramatic acceleration of oxidation [77]. Such accelerated oxidative degradation is one of the

most serious reasons for slow growth of industrial applications of nanocomposites [78].

Stabilizers are a kind of additives, which endow high photo- and thermoxidative stability to polymer. The efficiency of stabilizers depends on many factors such as the chemical activity of functional groups, the compatibility, diffusivity, and volatility of stabilizers in polymer matrices. That is, even with a high chemical activity, a stabilizer must not be effective unless it is molecularly dispersed, facilely migrates to an oxidizing area, and is well retained in the polymer matrix without being lost. Especially, the retention of a stabilizer is one of the most important factors for long-term stabilization of PP, since a stabilizer is gradually lost to atmosphere. Recently, we reported that loosely connected interfaces formed between PP and filler accelerate the physical loss of stabilizers from the interfaces, which is believed as one of major factors for inorganic filler to destabilize PP [79].

Dendritic polymer exhibits specific properties due to its globular and highly functional structure, leading to a variety of potential applications [80]. Especially, its open interior space can be applied to drug delivery and releasing applications, where drug molecules are encapsulated in an interior space through non-bonded attraction [81]. We thought that such a characteristic of dendritic polymer might be useful for the retention of stabilizers, where it was expected that dendritic polymer carries, disperses and retains stabilizers in PP-based nanocomposites. The purposes of this study were to introduce branched polyglycidol (PGL) on SiO_2 nanoparticles via anionic ring-opening polymerization and to study the influence of the topology of the grafted PGL (linear, brush and dendritic) on the thermoxidative stability of PP/SiO_2 nanocomposites. Anomalous stabilization was achieved when dendritic PGL was introduced.

4.2. Experimental section

Materials

Glycidol (purity 98%, Sigma-Aldrich Corporation) and toluene (Kanto Chemical Co., Inc.) were used after being dried over molecular sieves 4A or 13X followed by N_2 bubbling for 3 h, respectively. SiO_2 nanoparticles (AEROSIL®300, the average diameter = 7 nm, the surface area = 300 m^2/g) were dried in vacuum at 200°C before the usage. PP pellets (Novatec™ FY4) of M_w = 3.2 x 10^5 g/mol and M_w/M_n = 4.2 as a matrix were donated from Japan Polypropylene Co., Ltd. n-Octadecyl-3-(4'-hydroxy-3',5'-di-*t*-butylphenyl)propionate (AO-50) as a stabilizer was donated from ADEKA Corporation.

Synthesis of PGL-grafted SiO_2 nanoparticles

PGL with different topologies on SiO_2 nanoparticles was synthesized via anionic ring-opening polymerization based on literature [82] (Scheme 4.1). Briefly, 1.0 g of SiO_2 nanoparticles was deprotonated with 55.1 mg of sodium methoxide in 4.0 ml of anhydride methanol at room temperature overnight. After drying, the deprotonated SiO_2 was soaked in 10 ml of toluene and 5.0 ml of glycidol under N_2, and the polymerization was implemented at 110°C for 2 h. The reaction slurry was poured into methanol, filtered, and dried in vacuum. In this way, linear PGL (the 1st generation) was synthesized with one OH left as branches. The obtained linear PGL-grafted SiO_2 was termed G1-*g*-SiO_2 according to the generation. 1.0 g of

G1-*g*-SiO_2 was similarly deprotonated with sodium methoxide, and subjected to the second polymerization using 5.0 ml of glycidol in 10 ml of toluene. Since the polymerization initiates not only from the terminal ONa but also from ONa at the branches, a brush structure was obtained as G2-*g*-SiO_2. The same procedure starting from G2-*g*-SiO_2 led to G3-*g*-SiO_2 with a dendritic structure, where the majority of the polymerization was performed at the branches of the branches.

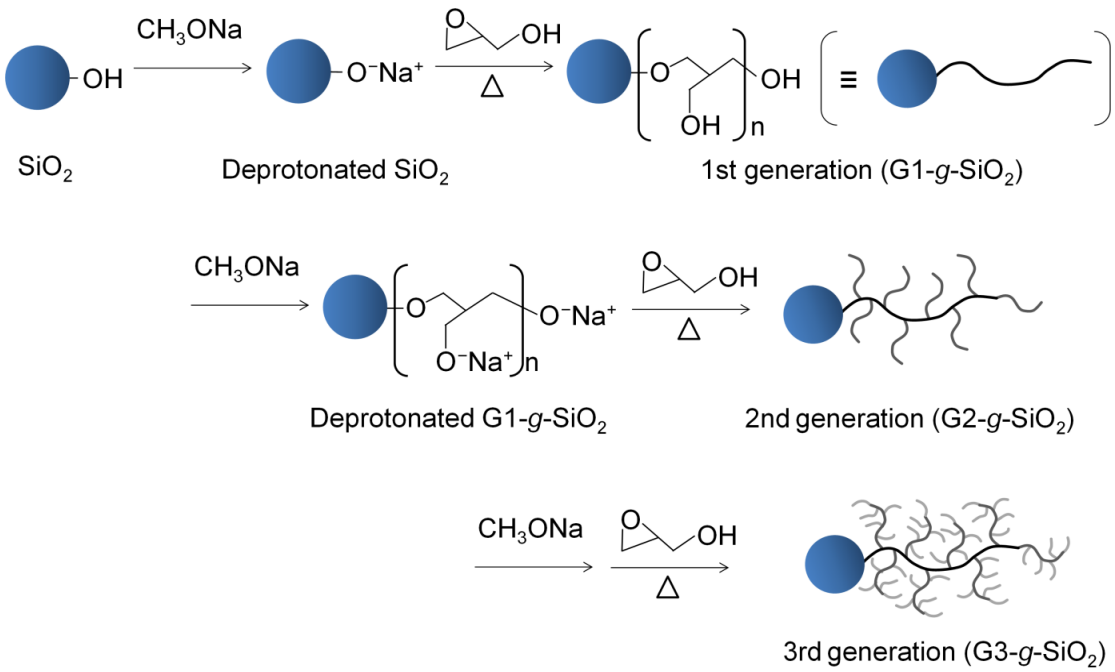

Scheme 4.1. Stepwise grafting of PGL to SiO_2 nanoparticles

Preparation of nanocomposites

Nanocomposites were prepared by melt mixing using a two-roll mixer at 20 rpm. PGL-grafted SiO_2 (whose amount was set to 1.0 wt% in terms of the SiO_2 weight) and

AO-50 (0.1 wt%) were added to the PP pellets that were preliminarily kneaded at 185°C for 5 min. The mixture was kneaded at 185°C for additional 10 min. Thus prepared nanocomposites were hot-pressed into sample films with the thickness of 100 μm at 230°C and 10 MPa, and then quenched at 100°C.

Characterizations

Transmission Fourier-transform infrared (FT-IR) spectra were acquired on JASCO FT/IR-6100 in the rage of 800-4000 cm^{-1} to confirm the formation of PGL on SiO_2 nanoparticles. FT-IR specimens were prepared as KBr discs. The amount of grafted PGL was measured by thermogravimetric analysis (TG, Mettler TG50), where the temperature was first kept at 200°C for 30 min to remove physisorbed water, and then ramped up to 650°C at a rate of 20 °C/min under dry air flow at 50 ml/min. The grafted amount was calculated by the weight loss from 200 to 650°C, in which unmodified SiO_2 nanoparticles exhibited negligible weight loss. The sample crystallinity was measured by differential scanning calorimetry (DSC, Mettler Toledo DSC 822) based on the following equation.

$$\text{Crystallinity (wt\%)} = \frac{\Delta H}{\Delta H_0} \times 100$$

where ΔH is the total exotherm for the crystallization of a sample and ΔH_0 is a reference value (209 J/g) for 100% crystalline PP [81]. A specimen was placed in a sealed aluminum pan and then heated from 35 to 200°C at 10 °C/min under N_2 flow at 75 ml/min. The thermoxidative degradation was conducted and *in-situ* detected using a chemiluminescence (CL) analyzer (Tohoku Electronic Industrial Co., Ltd.,

CLA-ID2-HS). A sample film of 6.0 φ was placed on an aluminium pan and kept at 180°C under dry air flow at 100 ml/min. The thermoxidative stability of a sample was defined as oxidation induction time (OIT), which is the time till the initiation of the auto-oxidation. At least, two measurements per sample were performed to acquire the average OIT value.

4.3. Results and Discussion

Characterization of PGL-grafted SiO_2 nanoparticles

Figure. 4.1 shows FT-IR spectra for PGL-grafted SiO_2 nanoparticles at different generations.

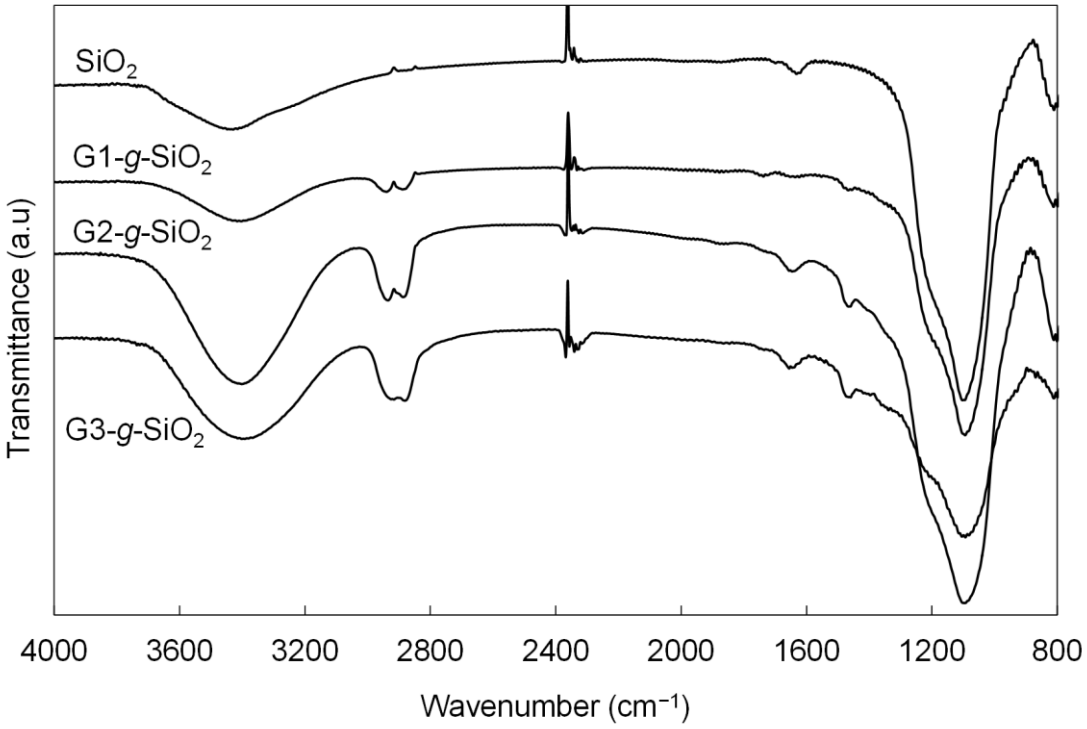

Figure 4.1. FT-IR spectra of SiO_2 and PGL-grafted SiO_2 nanoparticles

The spectroscopic evidence supported the formation of PGL on the SiO_2 surfaces. The peak at 1420 cm^{-1} is attributed to the C-O-H bending vibration in the PGL chain. The presence of numerous hydroxyl groups was also indicated by a large O-H stretching band at 3500 cm^{-1} mainly due to H-bonded hydroxyl groups of PGL and a small amount

of physisorbed water, which was indicated in TG measurements (described later). The absorption bands located at 2880 and 2930 cm^{-1} corresponded to the C-H stretching vibration of -CH_2- groups in PGL attached to the SiO_2 surfaces. All these absorption bands relevant to the PGL formation were enhanced as the generation grew. In this way, stepwise polymerization of glycidol was successfully performed on the SiO_2 surfaces.

TG measurements were conducted to evaluate the grafted amounts of PGL to SiO_2 nanoparticles (Figure 4.2).

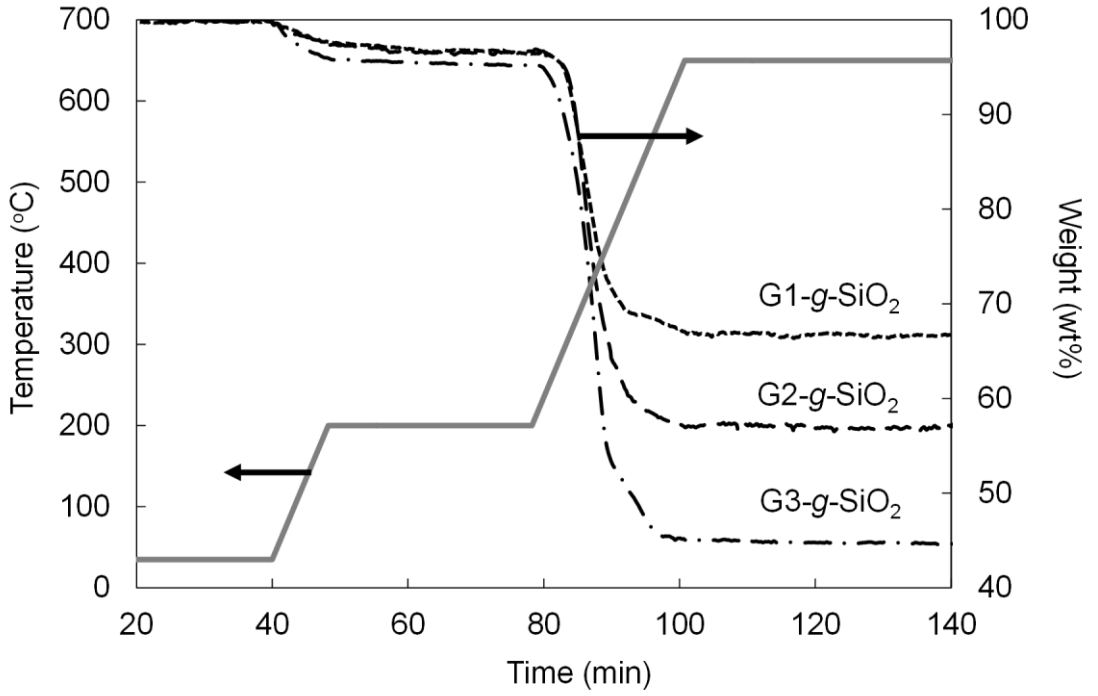

Figure 4.2. TG curves for PGL-grafted SiO_2 nanoparticles

Followed by the desorption of physisorbed water (about 3-4 wt%), significant weight loss was observed between 300 and 400°C for the PGL-grafted SiO_2 nanoparticles. Since pristine SiO_2 did not show such great loss in the same range, the

observed loss was clearly attributed to the presence of grafted PGL. Consistent to the IR results, the amount of grafted PGL increased at a higher generation. The amount of grafted PGL was respectively estimated as 29.9, 41.1 and 51.8 wt% for G1-, G2- and G3-*g*-SiO_2. 29.9 wt% for G1-*g*-SiO_2 indicated that 7.7% of 5.0 ml of glycidol was grafted in the first polymerization. Similarly, the second and third polymerization gave the grafting of 6.1% and 3.5% of the monomer. Thus, the grafting efficiency of glycidol decreased as the generation grew: The stepwise polymerization made surfaces more and more crowded, and consequently the diffusion of the monomer to the growth fronts was perturbed. A similar phenomenon was observed when terminally functionalized polymer was grafted to SiO_2 surfaces [34]. In summary, PGL grafting to SiO_2 nanoparticles via stepwise polymerization of glycidol was successfully accomplished.

Properties of PP/PGL-grafted SiO_2 nanocomposites

The crystallinity and the melting temperature of the PP/PGL-grafted SiO_2 nanocomposites were measured by DSC (Table 4.1). The crystallinity and the melting temperature were not largely affected by the addition of PGL-grafted SiO_2 irrespective of the PGL topology. CL profiles during the thermoxidative degradation at 180°C are reported in Figure 4.3, and the average OIT values are summarized in Table 4.1.

Table 4.1. Crystallinity, melting temperature and average OIT of PP and PP/PGL-grafted SiO_2 nanocomposites

Sample	Crystallinity (wt%)	Melting temperature (°C)	Average OIT (h)
PP	47.3	164.5	15.5
PP/G1-*g*-SiO_2	48.3	162.6	16.5
PP/G2-*g*-SiO_2	47.6	163.3	17.2
PP/G3-*g*-SiO_2	49.2	162.3	23.0

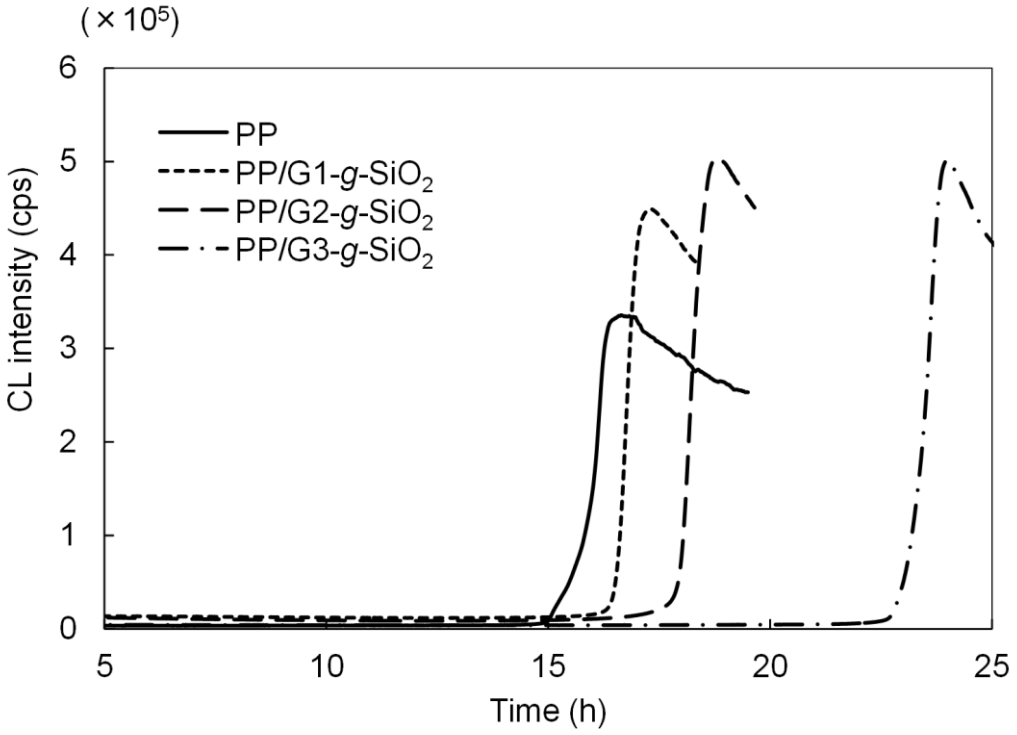

Figure 4.3. CL profiles for PP and PP/PGL-grafted SiO_2 nanocomposites

It was found that the addition of 1.0 wt% of G1- and G2-*g*-SiO_2 slightly increased OIT by about 1 h and 2 h as compared with PP, respectively. In contrast, the addition of G3-*g*-SiO_2 caused an anomalous OIT improvement by about 7 h. It is notable that G3-*g*-SiO_2 possessed surface PGL chains similar to the other generations, and that the PGL amount increased only by 10 wt% from G2-*g*-SiO_2. The only and the biggest difference is the topology of the grafted PGL chains. As can be seen from the OIT values for G1- and G2-*g*-SiO_2, the chemical structure of PGL must not have a stabilizing effect for PP. Therefore, it was presumed that dendritic PGL for G3-*g*-SiO_2 might interact with the stabilizer (AO-50) in a way to improve its efficiency. As was mentioned in the introduction, dendritic polymer has been frequently employed for molecular encapsulation, while it is not the case for brush polymer. Consequently, the

most plausible scenario was that dendritic PGL on SiO_2 surfaces might entrap and retain the stabilizer molecules in its interior in order to prevent the physical loss of the stabilizer. Even separately from the exact mechanism, the observation that surface dendritic polymer grafted to nano-sized filler significantly enhanced the thermoxidative stability of PP has never been reported and believed as a promising way for elongating the lifetime of nanocomposites.

4.4. Conclusion

In this work, polyglycidol (PGL) chains were grafted to SiO_2 nanoparticles via stepwise anionic ring-opening polymerization. PGL chains with different topologies were successfully introduced, and resultant PGL-grafted SiO_2 nanoparticles were melt mixed with polypropylene (PP) to obtain nanocomposites. While the chemical structure of PGL itself did not have any stabilizing effect, the topology of PGL significantly affected how PGL interacted with a hindered phenol stabilizer: Dendritic PGL caused anomalous enhancement of the thermoxidative stability of PP/SiO_2 nanocomposites, plausibly due to encapsulation of the stabilizer inside the interior space of the dendritic structure. The obtained results are not only effective but also new in achieving long-term use of PP nanocomposites. Further, the same idea might be applicable for enhancing the effectiveness of other molecular additives.

Chapter 5

Long-term Stability for Capacitor Applications by Controlling Crystal Morphology

5.1. Introduction

The application area of PP has been expanded with increasing its productions because of its balanced properties. Recently, specialty classes of PP materials are focused on as future promising materials. For example, capacitor application is one of the most attentional fields as a research area for PP materials because it can fully utilize the performance of insulation properties of PP.

In industrial field, this capacitor has been mainly developed in automobile fields. And this field will develop as electrical automobiles in the future. Its desirable ability for PP is mainly the thickness and long-term stability. Developments of processing ability have been contributed the preparation of polymer thin film for capacitor application. According to industry, the thickness of PP film became almost less than 3 μm in these last few years as I mentioned in general introduction. When we make PP film thinner, it is getting harder without clarify the structure property relationship. And also the long-term stabilization of PP film is necessary for understanding of its mechanism.

Recently, some researchers found that the relationship between crystalline diameter of PP and its property of electrical breakdown voltage (BDV). In this finding, it was clarified the smaller diameter of crystalline gives stronger BDV properties. As mentioned in Figure 5.1. This finding indicates the importance of morphology control of PP materials.

Improvement of BDV properties for capacitor application of PP was aimed in this chapter. In addition, a molecular mass dependence of crystallization in PP is not yet

well established. Therefore, crystalline structure was characterized by using various molecular weight of PP firstly.

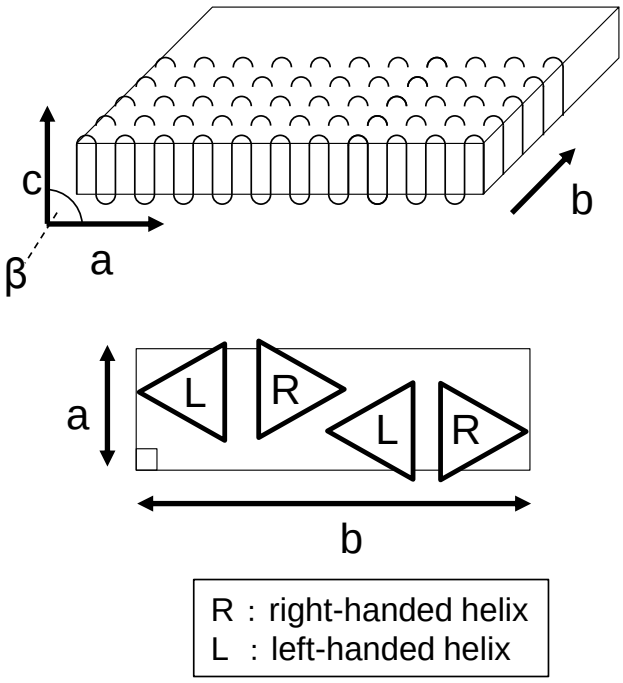

Figure 5.1. α crystal morphology of polypropylene.

5.2 Experimental Section

Materials

Table 5.1 shows the information of PP pellets used in this chapter. All the polymer pellets were homo and used as donated without any modification. The donation companies are non-disclosure.

Table 4.1. Sample information

Sample	M_n ($\times 10^4$)	M_w ($\times 10^4$)	MWD	*mmmm* (mol%)	MFR (g/10min)
Base-PP	3.6	31	8.6	95	4.6
A	4.5	34	7.5	96	3.4
B	12.0	58	4.8		0.35
C	7.5	37	4.9		1.9
D	12.0	50	4.4		0.5
E					3
F				96	5

Sample preparation

Base-PP pellet and sample A - F were melt-mixed using two-roll mixer at 185°C and 20 rpm for 5 min with 35 wt% of blend PPs. Sample films were prepared by hot press at 230°C and 10 MPa with the thickness of 200 μm. The films were then quenched at 100°C for 5 min, followed by quenching at 0°C.

Characterizations

The crystalline structures and crystallinities of the samples were evaluated by the wide-angle X-ray diffraction (WAXD). WAXD was performed on a X-ray diffractometer using the monochromated Cu Kα radiation at 30 kV and 20 mA.

5.3. Results and Discussion

Figure 5.2 shows the results of XRD measurements for characterize the crystalline type and crystallinity.

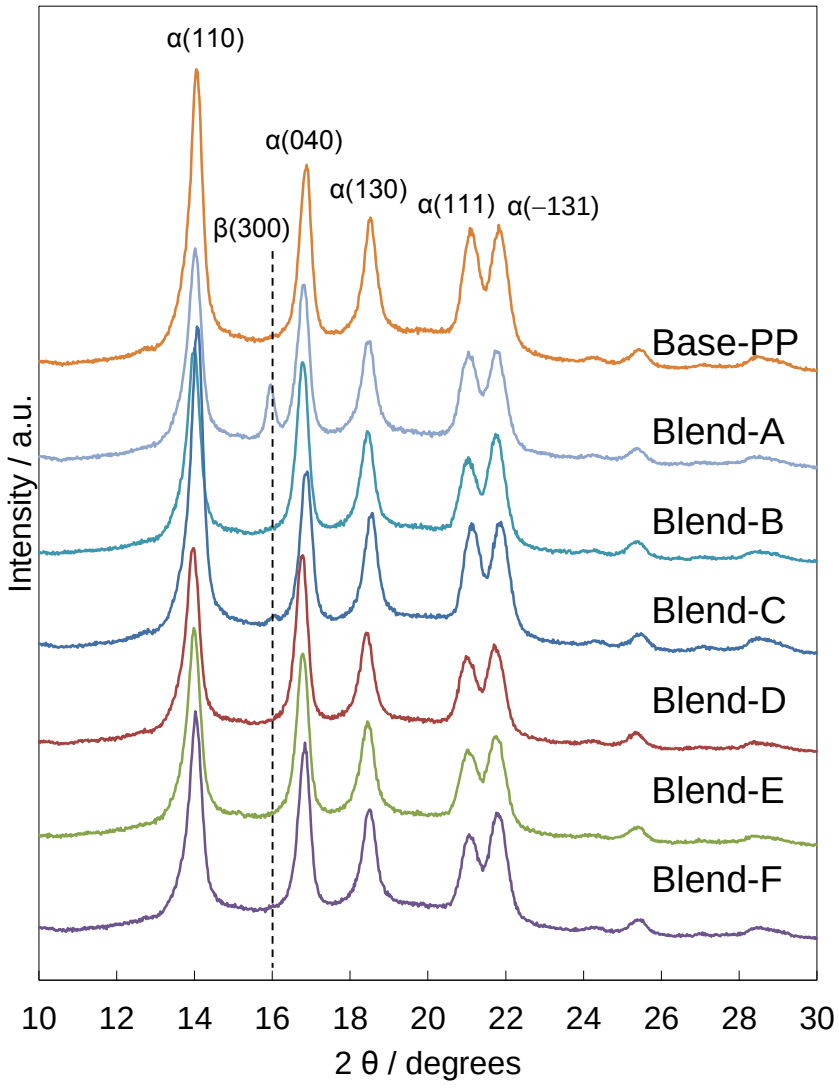

Figure 5.2. XRD pattern of each sample

Figure 5.2 shows mainly α-crystalline structure and some sample contains small

amount of β-crystal. Generally, biaxial drawing machine has been applied to prepare thin film for capacitor application. In this process,α-crystalline appears as a main crystal. Therefore, we plan to discuss durability of PP based on α form.

Table 5.2

Crystallinity from XRD mesurements

Sample	Total-crystallinity (vol%)	β-crystallinity (vol%)
Base-PP	57.3	0.0
Blend-A	55.2	2.3
Blend-B	56.1	0.0
Blend-C	57.0	0.2
Blend-D	53.5	0.0
Blend-E	55.5	0.0
Blend-F	57.1	0.0

BDV value is one of the most important factors to estimate their durability for capacitor application. Figure 5.3 shows the relationship between lattice constant and BDV value..

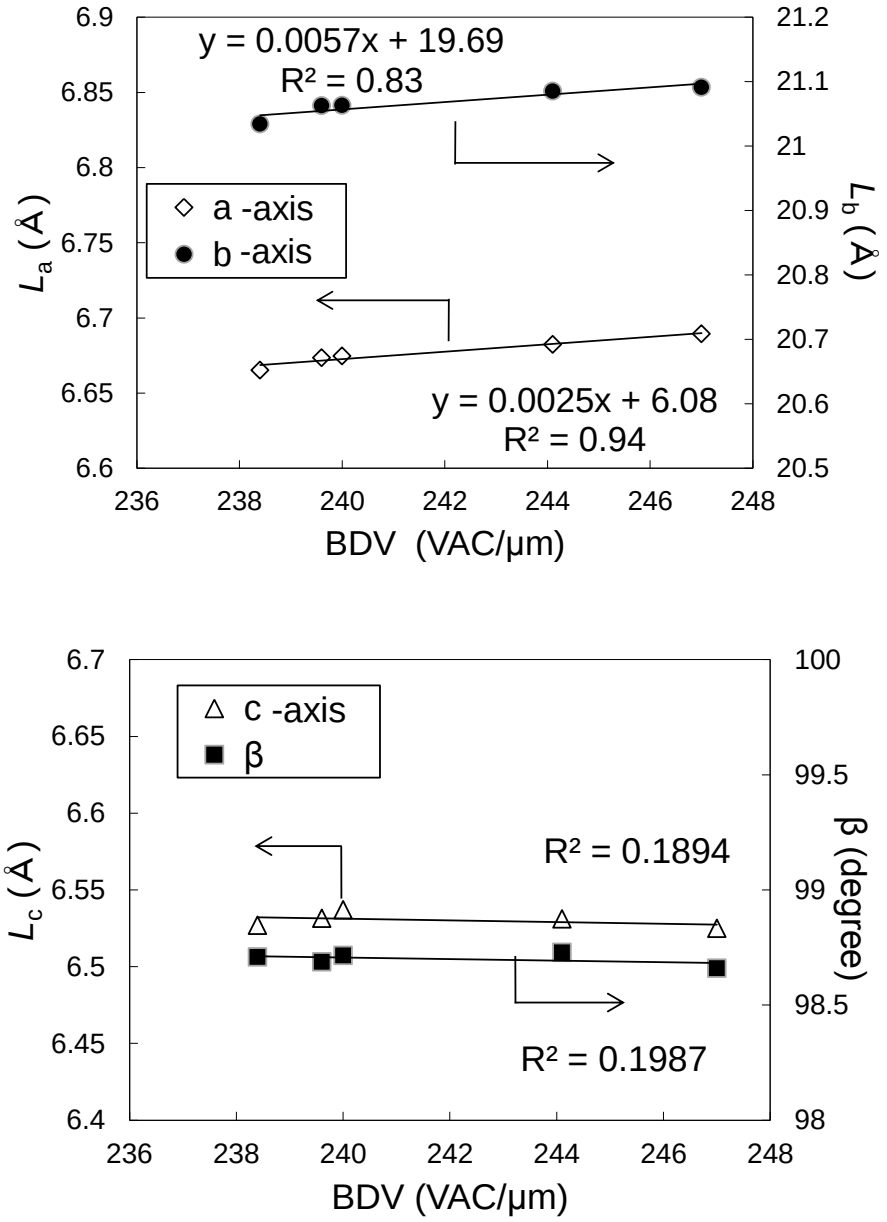

Figure 5.3. Relationship between BDV values and lattice constant (upper) a- and b-axis, (lower) c-axis and β degree

Figure 5.3 suggested that the a- and b-axis were well correlated with BDV value. This means we can estimate BDV value of PP films from lattice constants. However, c-axis and β degree showed no correlation with BDV value.

Chang et al. reported the effect of crystallization condition to its crystal lattice constants [83]. Figure 5.4 shows their report.

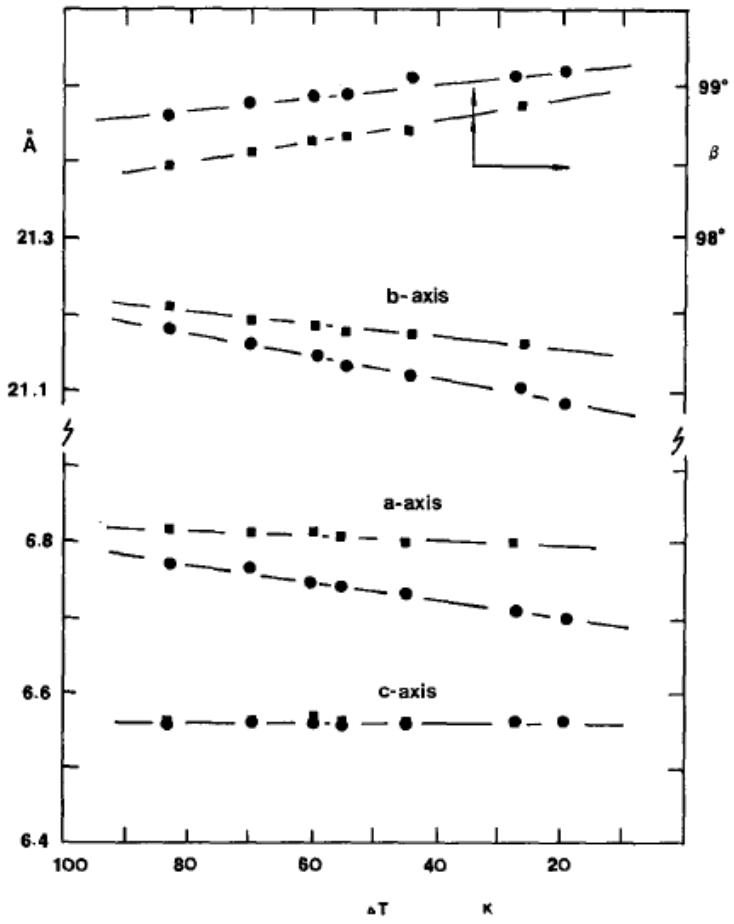

Figure 5.4 The crystal unit-cell parameter (a, b, c axis and β) for high-isotactic PP (●) and low-isotactic PP (■) change with supercooling

In their report, it was explained that the change of lattice constant by changing supercooling conditions from molten state. Lattice constant of PP crystal become smaller when supercooling speed was slower. It can be explained following. If crystallization speed was slower, PP can crystalize with fiberizing chain entanglements and form high dense crystal form. Their explanation was reasonable to conclude.

In this study, lattice constant of PP crystal had changed without changing crystallization condition but with changing PP pellets. This suggests that primary structure of PP well affects to PP lattice constant. It is highly possible that the molecular weight of PP is also affects BDV value but still now no report explain the relationship between primary structure and BDV value.

If we clarify the relationship among them, BDV can be easily predicted by designing polymer primary structures, which can control by olefin catalyst technology.

Figure 5.5 shows the relationship between lattice constant and molecular weight.

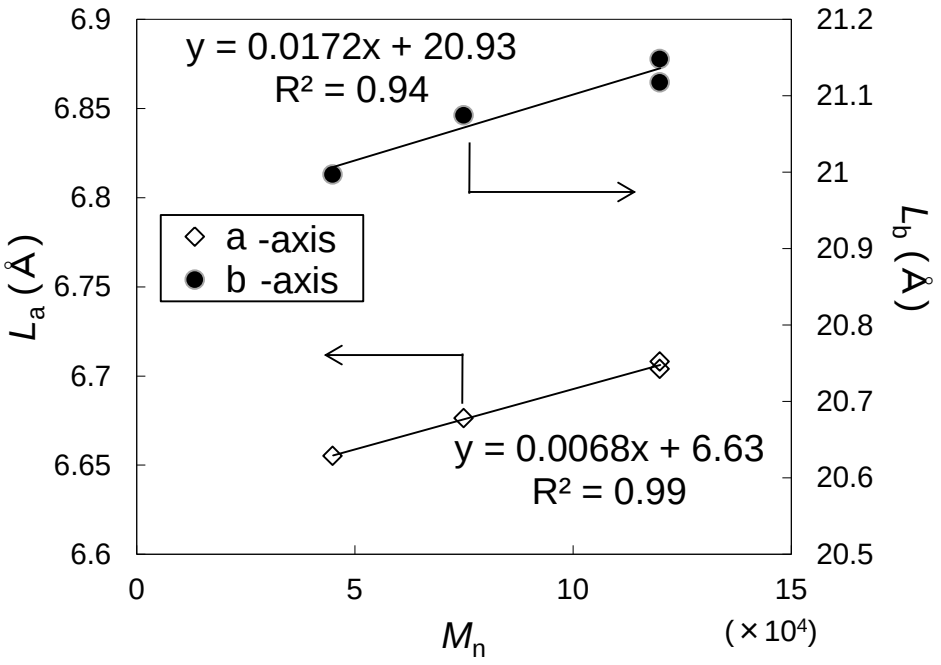

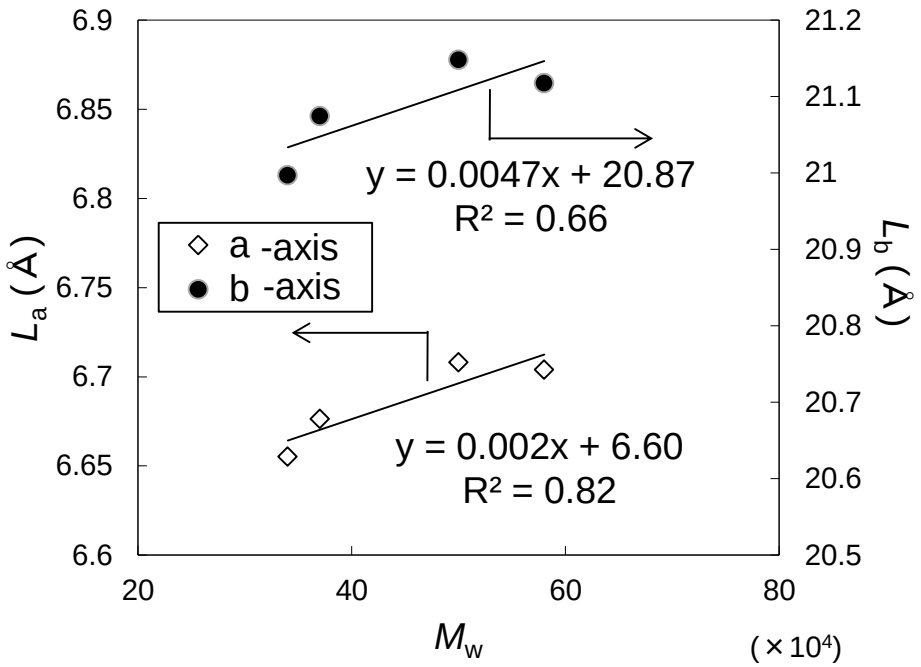

Figure 5.5. Crystal unit-cell parameters (a- and b-axis) with various molecular weights of blend PP

High correlation values were resulted from Figure 5.5. Especially, M_n shows higher correlation than M_w. This result can be explained by Chang's report. It is highly possible that PP is easy to crystalize when molecular weight is lower because of less entanglements.

Therefore, we can summarize these results as following Figure 5.6.

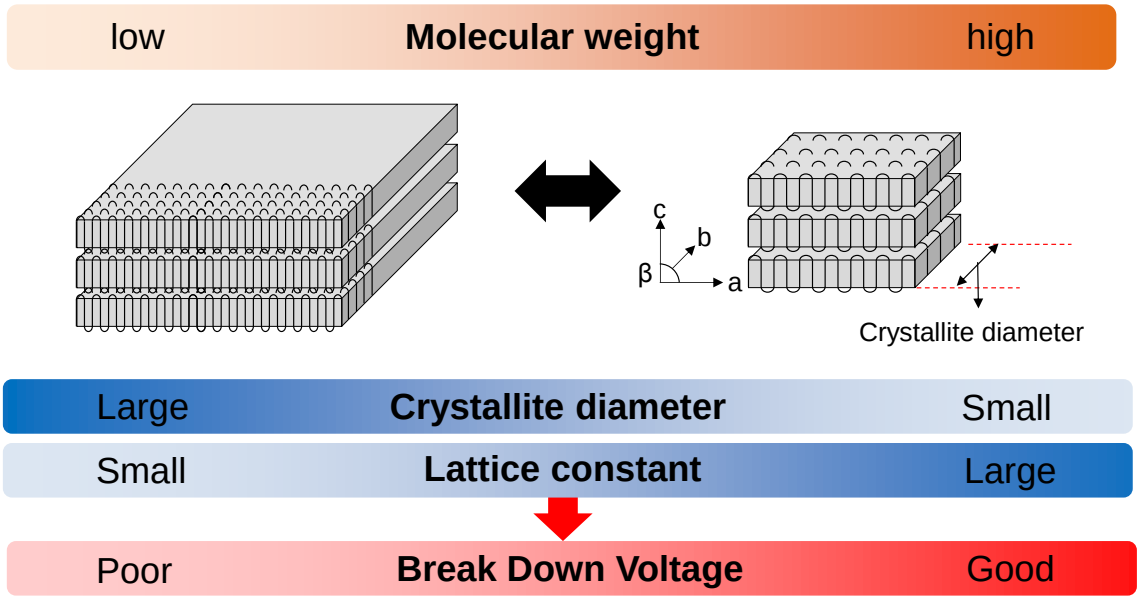

Figure 5.6 Summary of the relation between BDV value and other factors

This result clearly said that the relationship between BDV and high order structures of PP. Furthermore, molecular weight also affects BDV from this research. Therefore it was suggested that the primary structure of PP also strongly affects BDV value and we can control high order structure by designing primary structure of PP. For example, copolymerization is well affects crystalline structure of PP because of preventing lamella formation. And the addition of small amount of long chain branch highly effective for processing because of its high melt strength and strongly change crystalline structure because of its nucleation ability.

From Figure 5.5, we can estimate BDV values without measurements. Therefore, we tried to get some prediction of BDV values from lattice constants. For the prediction, we applied three kinds of blend polymer in this chapter. Table 5.3 shows the information of polymers.

Table 5.3

Polymer information

Sample	M_w ($\times 10^4$)	Details
HMW-PP	109	High molecular weight PP (synthesized in lab)
RPP	16	Ethylene propylene rubber (ethylene content 2.5%)
LB-PP	-	Long branch contained PP

Sample preparation was followed by same procedures but blend ration was changed to confirm the effects of blending amounts. Figure 5.7 shows the results of characterization.

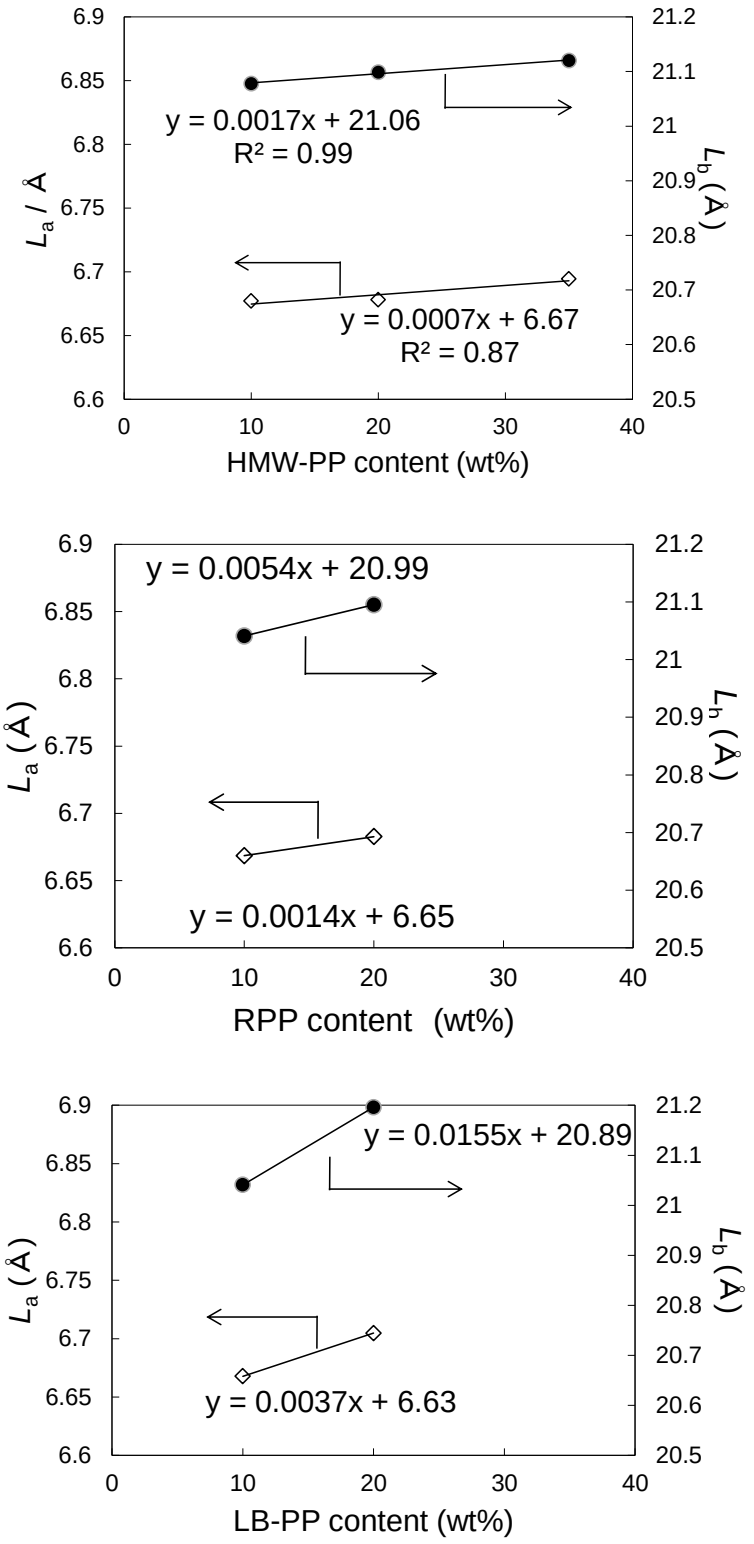

Figure 5.7. Relationship between lattice constant and blend polymer contents (upper) HMW-PP, (middle) RPP, (lower) LB-PP

Figure 5.7 gave us the correlation between lattice constant and blend polymer amount. The entire polymer shows increase of lattice constants with increase blend polymer amount. However, change of slope is depends on the kinds of polymer.

Figure 5.8 and 5.9 shows the prediction of BDV value.

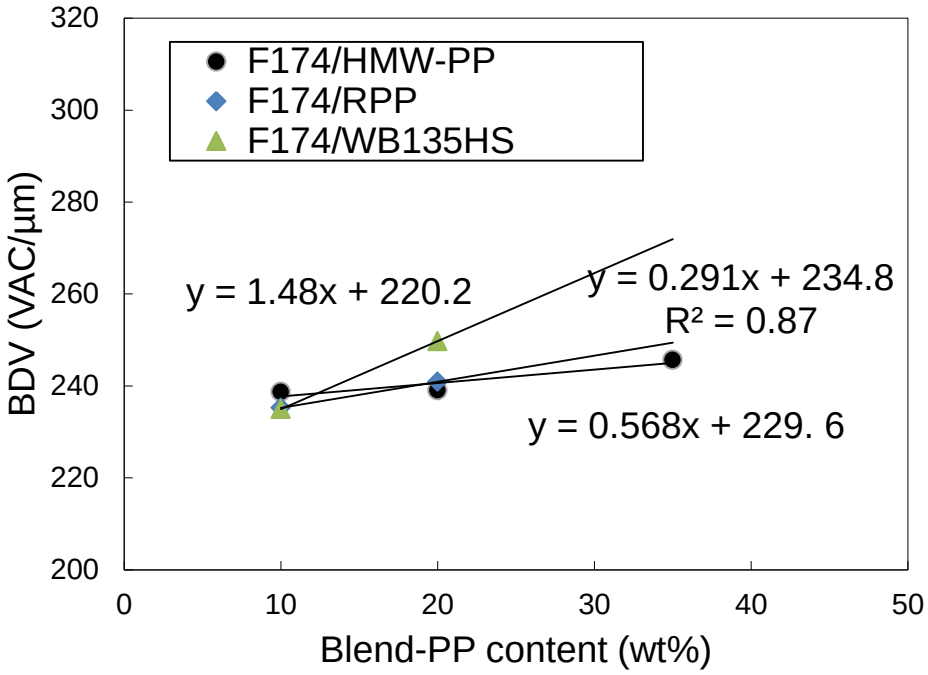

Figure 5.8. BDV prediction from unit-cell parameter (a-axis)

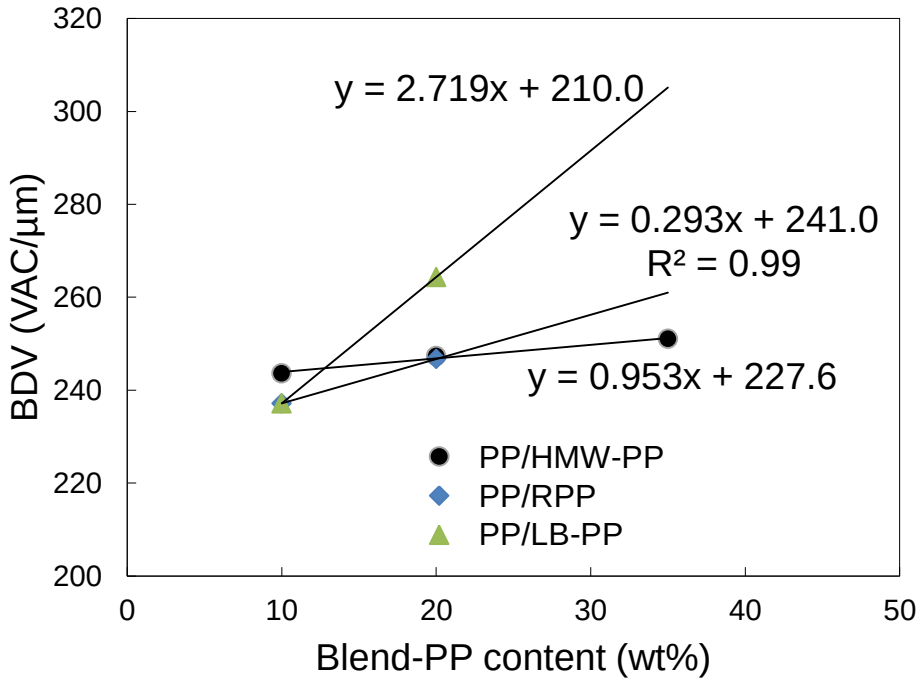

Figure 5.9. BDV prediction from unit-cell parameter (b-axis)

Both a- and b-axis can predict BDV value from Figure 5.8 and 5.9. It can conclude that the understanding of the relationship between high-order structure and their durability can predict higher performance design for next stage. Especially, LB-PP is the highest improvements of BDV form this prediction. In the case of HMW-PP, even 10 wt% of blending is more effective than other polymers. As results, the controlling of primary structure was useful for design these properties.

5.4. Conclusion

In this chapter, the crystal unit-cell parameters were observed with changing molecular mass by wide-angle X-ray diffraction (WAXD) to predict BDV value for long-term application as capacitors. Figure 5.2 showed that all the samples have mainly α-crystal form from WAXD measurements. Figure 5.3 indicates good correlation between crystal unit-cell parameters (a- and b-axis) and molecular number (M_n). High M_n samples might have lower density crystal unit-cell because it is difficult for them to reduce their entanglements. Then the BDV value predictions were achieved by using crystal unit cell. As a conclusion, it is the first report about the relationship between lattice constant and BDV values of PP materials.

Chapter 6

General conclusion

6.1 General Summary

The objective of this research is to improve the life-time of PP materials by encapsulation and morphology control. Chapter 2 showed the G4-HBP effectiveness in PP matrix and it was discussed in its stabilization mechanism. Chapter 3 showed the generation effect for stabilization and applicant for PP nanocomposites. Chapter 4 showed the improvements and prediction of PP film durability for long term capacitor application.

In chapter 2, The G4-HBP effects for the stabilization of PP materials were researched and discussed. The highly stabilized PP material was prepared by addition of G4-HBP. It was confirmed that the G4-HBP has no stabilization ability itself and the volatilization of antioxidants from PP matrix was suppressed by G4-HBP. These results suggest that the G4-HBP play as a molecular encapsulation. And also the antioxidants structure might be affect to OIT improvement. Especially, the presence of ester bond in antioxidants might be the key for this stabilization.

A highly stable PP nanocomposite was prepared successfully by applying a new stabilization technology using HBP in chapter 3. It was discovered that the addition of HBP is useful for the stabilization of not only PP but also PP nanocomposites. Especially, the stability of a PP/SiO_2 nanocomposite was significantly improved by a synergetic effect plausibly due to in-situ grafting of HBP to SiO_2 during melt-mixing.

In chapter 4, polyglycidol (PGL) chains were grafted to SiO_2 nanoparticles via stepwise anionic ring-opening polymerization. PGL chains with different topologies were successfully introduced, and resultant PGL-grafted SiO_2 nanoparticles were melt mixed with PP to obtain nanocomposites. While the chemical structure of PGL itself

did not have any stabilizing effect, the topology of PGL significantly affected how PGL interacted with a hindered phenol stabilizer: Dendritic PGL caused anomalous enhancement of the thermoxidative stability of PP/SiO_2 nanocomposites, plausibly due to encapsulation of the stabilizer inside the interior space of the dendritic structure. The obtained results are not only effective but also new in achieving long-term use of PP nanocomposites. Further, the same idea might be applicable for enhancing the effectiveness of other molecular additives.

In chapter 5, the crystal unit-cell parameters were observed with changing molecular mass by wide-angle X-ray diffraction (WAXD) to predict BDV value for long-term application as capacitors. All the samples have mainly α-crystal form from WAXD measurements in chapter 5. And also it was indicated good correlation between crystal unit-cell parameters (a- and b-axis) and molecular number (M_n). High M_n samples might have lower density crystal unit-cell because it is difficult for them to reduce their entanglements. Then the BDV value predictions were achieved by using crystal unit cell. As a conclusion, it is the first report about the relationship between lattice constant and molar mass fraction in PP.

This doctoral dissertation is about long-term application of PP materials. The results in this study are remarkably important for the total understandings of the long-term stabilization of PP to design novel approach. The knowledge obtained in this study will contribute to the further development of PP materials and the expansion the application area of PP.

Reference

[1] R. B. Saymour, C. Vasile, M. Rusu, "Application of polyolefins", In: *Handbook of polyolefins.*

[2] J. M. Raquez, Y. Habibi, M. Murariu, P. Dubois, *Prog. Polym. Sci*., **2013**, *38*, 1504.

[3] Z. Qi, C. Jie, W. Tiejun, X. Ying, *Energy Convers. Manage*., **2007**, *48*, 87.

[4] S. P. Pyl, C. M. Schietekat, M.F. Reyniers, R. Abhari, G. B. Marin, K. M. V. Geema, *Chem. Eng. J*., **2011**, *176*, 178.

[5] R. J. Samuels, Structured Polymer Properties, *Wiley*, **1974**, New York

[6] G. Natta, P. Corradini, J. Polym. Sci., **1959**, *39*, 29.

[7] G. Natta, P. Corradini, *Nuovo Cimento, Suppl*., **1960**, *15*, 9.

[8] G. Natta, P. Corradini, P. Ganis, *Makromolekulare Chemie*, **1960**, *39*, 238.

[9] G. Natta, P. Corradini, P. Ganis, *J. Polym. Sci*., **1962**, *58*, 1191.

[10] G. Natta, G. Dall'Asta, G. Mazzanti, et al., *Makromolekulare Chemie*, **1962**, *54*, 95.

[11] G. Natta, P. Corradini, *Nuovo Cimento, Suppl*., **1960**, *15*, 40.

[12] A. Turner-Jones, J. M. Aizlewood, D. R. Beckett, *Makromolekulare Chemie*, **1964**, *75*, 134.

[13] H. D. Keith, Jr, F. J. Padden, N. M. Walker, H. W. Wyckoff, *J. Appl. Phys*., **1959**, *30*, 1485.

[14] A. Turner-Jones, A. J. Cobbold, *J. Polym. Sci., Part B*, **1968**, *6*, 539.

[15] D. R. Morrow, B. A. Newman, *J. Appl. Phys*., **1968**, *39*, 4944.

[16] J. L. Kardos, A. W. Christiansen, E. J. Baer., *J. Polym. Sci., Part A2*, **1966**, *4*, 777.

[17] J. A. Sauer, K. D. Pae, *J. Appl. Phys*., **1968**, *30*, 4950.

[18] E. J. Addink, J. Bientema, *Polymer* **1961**, *2*, 185.

[19] A. Turner-Jones, J. M. Aizlewood, Beckett, D. R. *Makromolekulare Chemie*., **1964**, *75*, 134.

[20] G. Natta, P. Corradini, *Nuovo Cimento, Suppl*., **1960**, *15*, 40.

[21] M. Hikosaka, T. Seto, *J. Polym*, **1973**, *5*, 111.

[22] R. H. Olley, D. C. Bassett, *Polymer*, **1989**, *30*, 399.

[23] B. Lots, J. C. Wittmann, *J. Polym. Sci*., *Polym. Phys. Edd*., **1986**, *24*, 1541.

[24] R. I. Jose, M. Leo, J. G. Maria, G. A. Rufina, *J. Polym. Sci. Part B Polm. Phys.* **1998**, *37*, 323.

[25] Y. Fukushima, A. Okada, M. Kawasumi, T. Kurauchi, O. Kamigaito, *Clay Miner*., **1988**, *23*, 27.

[26] A. Usuki, Y. Kojima, M. Kawasumi, A. Okada, Y. Fukushima, T. Kurauchi, O. Kamigaito, *J Mater. Res*., **1993**, *8*, 1179.

[27] G. E. Padawer, N. Beecher, *Polym. Eng. Sci*., **1970**, *10*, 139.

[28] J. Lusis, R. T. Woodhams, M. Xanthos, *Polym. Eng. Sci*., **1973**, *13*, 139.

[29] S. Cai, G. Ji, J. Fang, G. Xue, *Angew. Macromol. Chem*., **1990**, *179*, 77.

[30] A. Garton, S. W. Kim, D. W. Wiles, *J. Polym. Sci*., *Polym. Lett. Ed*., **1982**, *20*, 273.

[31] M. Kawasumi, N. Hasegawa, M. Kato, A. Usuki, A. Okada, *Macromolecules*, **1997**, *30*, 6333.

[32] H. Lee, P. D. Fasulo, W. R. Rodgers, D.R. Paul, *Polymer*, **2005**, *46*, 11673.

[33] H. Lee, P. D. Fasulo, W. R. Rodgers, D.R. Paul, *Polymer*, **2006**, *47*, 3528.

[34] T. Taniike, M. Toyonaga, M. Terano. *Polymer*, **2014**, *55*, 1012.

[35] P. Gijsman, G. Meijers, G. Vitarelli, *Polym. Deg. Stab*., **1999**, *65*, 433.

[36] S. Al-Malaika, *Adv. Polm. Sci*., **2004**, *169*, 121.

[37] K. Jagadeesh, Mannekote, V. Satish, Kailas, *J. Mater. Res. Tecnol*., **2012**, *1(2)*, 91-95.

[38] M. Blumberg, C. R. Boss andJ. C. W. Chien, *J. Appl. Polym. Sci*., **1965**, *9(12)*, 3837.

[39] J. Holcik, M. Karvas, D. Kassovicova, J. Durmis, *Eur. Polym. J*., **1976**, *12*, 173.

[40] B. W. Evans, G. Scott, *Eur. Polym. J*., **1974**, *10*, 453.

[41] R. Pfaendner, *Polym. Deg. Stab*., **2010**, *95*, 369.

[42] S. M. Therias, B. Mailhot, D. Gonzalez, J. L. Gardette, *Chem. Mater*., **2005**, *17*, 1072.

[43] T. Taniike, M. Umemori, H. Chiba, K. Takeuchi, M. Terano, *J. Mater. Life Soc*., **2012**, *24*, 102.

[44] X. Gao, G. Hu, Z. Qian, Y. Ding, S. Zhang, D. Wang, M. Yang, *Polymer*, **2007**, *48*, 7309.

[45] X. Gao, X. Meng, H. Wang, B. Wen, Y. Ding, S. Zhang, M. Yang, *Polym. Deg. Stab*., **2008**, *93*, 1467.

[46] J. Chen, M. S. Yang, S. M. Zhang, *Compos. Part A Appl. Sci. Manuf*., **2011**, *42*, 471.

[47] S. Xu, Y. Luo, R. Haag, *Macromol. Biosci*., **2007**, *7*, 968.

[48] K. Inoue, *Prog. Polym. Sci*., **2000**, *25*, 453.

[49] J. Lange, E. Stenroos, M. Johansson, E. Malmstrom, *Polymer*, **2001**, *42*, 7403.

[50] A. Carlmark, C. Hawker, A. Hult, M. Malkoch, *M. Chem. Soc. ReV*., **2009**, *38*, 352.

[51] C. Gao, D. Yan, *Prog. Polym. Sci*., **2004**, *29*, 183.

[52] C. R. Yates, W. Hayes, *Eur. Polym. J*., **2004**, *40*, 1257.

[53] B. I. Voit, *J. Polym. Sci., Part A: Polym. Chem*., **2000**, *38*, 2505.

[54] H. Frey, R. Haag, *ReV. Mol. Biotech*., **2002**, *90*, 257.

[55] J. Vukovic, S. Jovanovic, M. D. Lechner, V. Vodnik, *J. Appl. Polym. Sci*., **2009**, *112*, 2925.

[56] C. Gao, D. Yan, *Prog. Polym. Sci*., **2004**, *29*, 183.

[57] P. Kesharwani, K. Jain, N. K. Jain, *Prog. Polym. Sci*., **2014**, *39*, 268.

[58] H. Bergenudd, P. Eriksson, C. D. Armitt, B. Stenberga, E. M. Jonsson, *Polym. Deg. Stab*., **2002**, *76*, 503.

[59] G. A. George, M. Celina, A. M. Vassallo, P. A. Cole-Clarke, *Polym. Deg. Stab*., **1995**, *48*, 199.

[60] J. Pospisil, W. D. Habicher, J. Pilar, S. Nespurek, J. Kuthan, G. O. Piringer, H. Zweifel, *Polym. Deg. Stab*., **2002**, *77*, 531.

[61] K. Sumino, T. Taniike, M. Terano, G. A. George, *Macromol. React. Eng*., **2008**, *2*, 135.

[62] H. Qin, C. Zhao, S. Zhang, G. Chen, M. Yang, *Polym. Deg. Stab*., **2003**, *81*, 497.

[63] H. Qin, S. Zhang, H. Liu, S. Xie, M. Yang, D. Shen, *Polymer*, **2005**, *46*, 3149.

[64] R. Pfaendner, *Polym. Deg. Stab*., **2010**, *95*, 369.

[65] M. Blumberg, C. R. Boss, J. C. W. Chien, *J. Appl. Polym. Sci*., **1965**, *9*, 3837.

[66] J. Holcik, M. Karvas, D. Kassovicova, J. Durmis *Euro. Polym. J*., **1976**, *12*, 173.

[67] M. Minagawa, *Polym. Deg. Stab*., **1989**, *25*, 121.

[68] N. Pasquini, A. Addeo, *Polypropylene Handbook*, **2005**.

[69] S. S. Ray, M. Okamoto, *Prog. Polym. Sci*., **2003**, *28(11)*, 1539.

[70] G. Choudalak, A. D. Gotsis, *Eur. Polym. J*., **2009**, *45(4)*, 967.

[71] M. Pöllänen, U. Pelz, M. Suvanto, T. T. Pakkanen, *J. Appl. Polym. Sci*., **2010**, *116(2)*, 1218.

[72] E. Pavlidou, D. Bikiaris, A. Vassiliou, M. Chiotelli, G. Karayannidis, *J. Phys*., **2005**, *10(1)*, 190.

[73] H. Zhao, R. K. Y. Li, *Polymer*, **2006**, *47(9)*, 3207.

[74] S. Morlat, B. Mailhot, D. Gonzalez, J. L. Gardette, *Chem. Mater*., **2004**, *16(3)*, 377.

[75] B. Mailhot, S. Morlat, J. L. Gardette, S. Boucard, J. Duchet, J. F. Gèrard, *Polym. Deg. Stab*., **2003**, *82(2)*, 163.

[76] H. Qin, S. Zhang, H. Liu, S. Xie, M. Yang, D. Shen, *Polymer*, **2005**, *46(9)*, 3149.

[77] S. Morlat, B. Mailhot, D. Gonzalez, J. L. Gardette, *Chem. Mater*., **2004**, *16(3)*, 377.

[78] R. Pfaendner, *Polym. Deg. Stab*., **2010**, *95(3)*, 369.

[79] T. Taniike, M. Umemori, H. Chiba, K. Takeuchi, M. Terano, *J. Mater. Life Soc*., **2012**, *24(3)*, 102.

[80] C. J. Hawker, J. M. J. Frechet, *J. Am. Chem. Soc*., **1990**, *112(21)*, 7638.

[81] A. K. Patri, I. J. Majoros, Jr. J. R. Baker, *Current Opin. Chem. Biol.*, **2002**, *6(4)*, 466.

[82] M. Khan, W. T. S. Huck, *Macromolecules*, **2003**, *36(14)*, 5088.

[83] S. Z. D. Cheng, J. J. Janimak, A. Zheng., *Polymer*, **1991**, *32(4)*, 648.

Achievements

Original Article

Ikki Katada, Minoru Terano, Toshiaki Taniike, “Stabilization of Polypropylene Nanocomposites by Dendritic Polyglycidol Modified Nano-Filler” *J. Mater. Life Soc.*, **2014**, accepted.

Ikki Katada, Masahito Toyonaga, Keisuke Goto, Fumihiro Kobayashi, Hibiki Chiba, Toshiaki Taniike, Minoru Terano, “Role of higher-order structures on the degradation and stabilization of polypropylene-based materials” *Kobunshi Ronbunshu*, **2013**, *70*, 693.

International conference

Ikki Katada, Toshiaki Taniike, Minoru Terano, “Antioxidants encapsulation for long-term stabilization of polypropylene materials by coexisting with hyperbranched polyester”, 248th ACS National Meeting and Exposition, 2014/08/10-14

Ikki Katada, Toshiaki Taniike, Minoru Terano, “Highly Stabilized Polypropylene Materials by Encapsulation of Antioxidants” International Symposium for Green-Innovation Polymers, 2014/03/06-07

Ikki Katada, Toshiaki Taniike, Minoru Terano, “New approach for highly stable polypropylene nanocomposites with synergistic effect of silica and dendritic polymer” 9th International Symposium on Weatherability, 2013/03/28-29

Ikki Katada, Toshiaki Taniike, Minoru Terano, “High stabilization effects of dendritic polyester for polypropylene nanocomposites” 4th International Conference on Polyolefin Characterization, 2012/10/21-24

Ikki Katada, Toshiaki Taniike, Minoru Terano, “Stabilization of polypropylene nanocomposites by fillers having surface dendritic polymers” 8th International Colloquium on Heterogeneous Ziegler-Natta Catalysts, 2012/03/27-30

Award

“多分岐ポリマーを用いたポリプロピレン系材料の安定化における安定化剤構造の影響”、 マテリアルライフ学会 第 24 回研究発表会、2013/07/05-06

Acknowledgments

I would like to express my sincere regards and gratitude to Professor Minoru Terano and Associate Professor Toshiaki Taniike for their invaluable guidance and support. This work would never have been performed without their help.

I also would like to express my sincere regards and gratitude to Dr. Tadakazu Miyata and Mr. Masahiro Nakata for their invaluable guidance and support.

I am greatly thankful to all the colleagues of Terano Laboratory for their biggest support and encouragement. I am also grateful to all the members of Terano and Taniike laboratories for being the best colleagues and for their immense cooperation during my stay in Terano Laboratory.

Ikki Katada

Terano Laboratory,

School of Materials Science,

Japan Advanced Institute of Technology

Minor Research Theme

Vibration Spectroscopic Analysis of Highly Stabilized Polypropylene Materials by Hyperbranched Polymer

by

Ikki Katada

Submitted to

Japan Advanced Institute of Science and Technology

1-1 Asahidai, Nomi, Ishikawa, 923-1292, Japan

Supervisor: Professor Graeme A. George

Professor of Polymer Science Chemistry

Queensland University of Technology, 2 George Street, Brisbane Qld 4001, Australia

【Introduction】

Polypropylene (PP) is one of the most widely used polyolefin because of its low cost, good processability, high chemical resistance, light weight, high melting point and well-balanced mechanical properties. However, PP is easy to degradate due to heat and light originally, and the addition of various antioxidants is essential in order to obtain practical stability. When considering the long-term usage of PP, not only the efficiency of the antioxidants but also the reduction of the physical loss of antioxidants, such as volatilization and leaching from PP matrix is important [1,2]. In addition, PP composite promotes volatilization of the antioxidant from the filler/matrix interface because of less interface adhesions [3]. Therefore, the suppressions of the volatilization and leaching of antioxidants are particularly important for PP materials. Addition of high molecular weight antioxidants is one of the general approaches. However, because of the low mobility of high molecular weight antioxidants, the combination with low molecular weight antioxidant is necessary.

In recent years, our group found that the stability of the PP is greatly improved by the addition of hyperbranched polymer (HBP) as molecular capsule [4]. It suggests that HBP significantly reduces the volatilization of the antioxidants without compromising the mobility of antioxidant. The merit of this method is to improve the efficacy of the conventional antioxidants without the synthesis new antioxidants. Meanwhile, the interaction between antioxidants and HBP has not been directly observed till now because of its difficulty.

The mechanism analysis of stabilization by HBP is focused in this minor research. It is difficult to characterize direct interaction between antioxidants and HBP in the PP matrix although it might be the key to establish this mechanism. Therefore, vibration

spectroscopic analysis like Fourier transform-infrared spectroscopy (FT-IR) and FT-IR emission has been used in this research.

【Experimental】

<Materials>

Unstabilized polypropylene powder polymerized by Ziegler-Natta catalyst was used as the matrix polymer (*mmmm* = 95 mol%, M_n = 57,000, M_w = 290,000, MWD = 5.02). *n*-octadecyl-3-(4'-hydroxy-3',5'-di-*t*-butylphenyl)propionate (ADEKASTAB AO-50) donated by ADEKA corporation was as an antioxidants. Hyperbranched *bis*-MPA polyester-64-hydroxyl, generation 4 (G4-HBP、M_w = 7323) was used as a molecular capsule. Figure 1 shows the structure of chemicals used in this study.

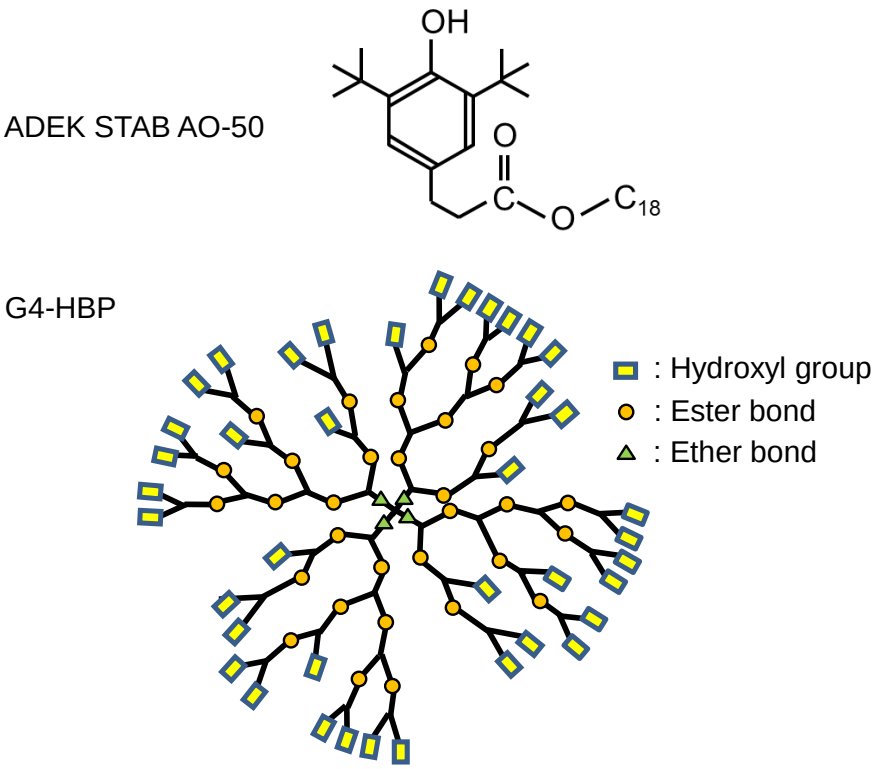

Figure 1. Chemical structures

<Experimental method>

①Sample preparation for FT-IR

To characterize the oxidation induction time (OIT) of PP in solid state, is more time consuming than in molten state because of low temperature (less than 165°C). In the main research, the amount of antioxidants has been controlled to estimate of polymer life more clearly. However, 0.07 wt% of antioxidants is too little to be estimated by analytical instruments (IR, UV-vis, etc.). In this study, the model samples containing 1.0 wt% of antioxidants were prepared to characterize the behavior of antioxidants in polymer matrix.

Four kinds of PP sample films were prepared for FT-IR (Scheme 1 and 2). Sample blending was performed by melt mixing with 1.0 wt% of AO-50 and/or 1.0 wt% of G4-HBP, respectively. The PP powder was blended in solid state with AO-50 before melt mixing. Blended PP powder was kneaded by two-roller mixer at 185°C for 5 min and then a given amount of G4-HBP was added into the kneaded PP. Melt mixing was performed in a corotating twin-roller. The mixture was kneaded at 185°C for another 10 min. The samples thus prepared were collected during the cooling process of the roller and subsequently stored in refrigerator.

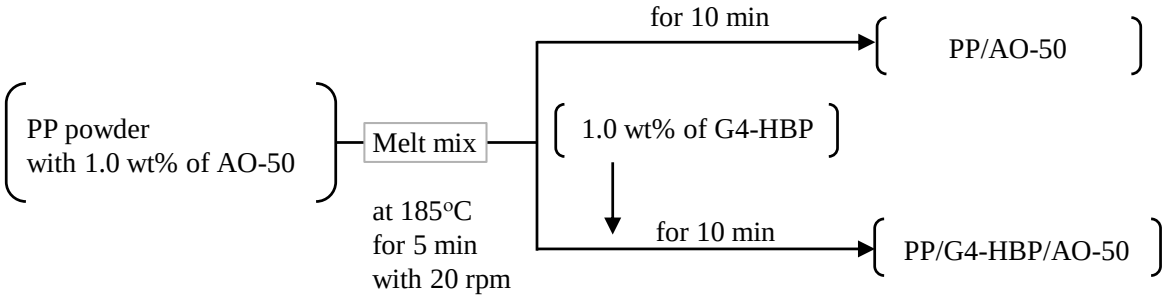

Scheme 1. Preparation of samples by melt-blending

After melt-mixing, the sample films were prepared (Scheme 2). Scheme 2 shows the procedure of film preparation. Blended samples were melted a t 230°C for 5 min and then pressed at 10MPa. Pressed samples were immediately annealed at 100°C for 5 min to keep same crystallinity of all the samples. Film samples thickness was kept constant (100 μm).

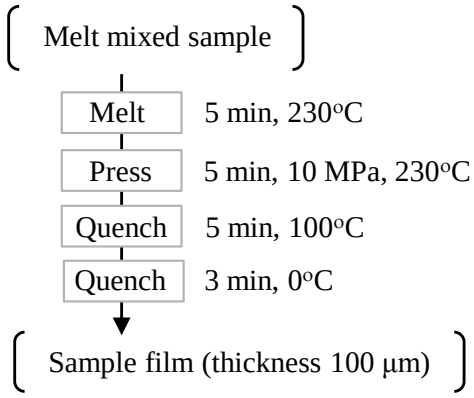

Scheme 2. Preparation of sample films

Table 1. Sample components for FT-IR

	PP (wt%)	AO-50 (wt%)	G4-HBP (wt%)
PP*[1]	100	-	-
PP/AO-50	99	1.0	-
PP/G4-HBP*[1]	99	-	1.0
PP/AO-50/G4-HBP	98	1.0	1.0

*[1] Antioxidants was extracted by hexane after film preparation.

Table 2. Measurement conditions of FT-IR

Temperature (°C)	27 (Room temperature)
Number of scans	64

②Sample preparation for FT-IR emission

The sample for FT-IR emission was prepared by diluting G4-HBP (10 mg) and/or AO-50 (10 mg) in 2.0 ml of methanol/acetone solution (1:1). After that, 8.0 μl of the mixture was dropped on the sample plate.

Table 3. Sample components for FT-IR emission

	AO-50 (wt%)	G4-HBP (wt%)
AO-50	100	-
G4-HBP	-	100
AO-50/G4-HBP	50	50

Generally, FT-IR measurements are used either in the reflective type or transmittance type. FT-IR emission is different from these measurements. It is much useful for real time quantitative analysis of samples. In the case of FT-IR emission, samples are needed in order to get infrared spectrum. The heated infrared spectrum corresponds to absorption spectrum. Thin films which are less than 2 μm are necessary for emission measurements.

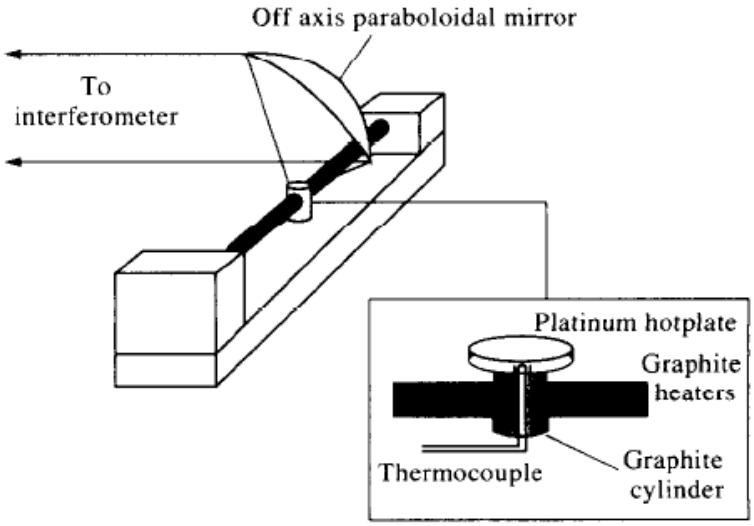

Figure 2. Schematic diagram of the emission cell used with the FT-IR spectrometer [5]

Table 4. Measurement conditions of FT-IR emission

Time (min)	180
Temperature (°C)	150
Flow rate (air, l/min)	12.0
Number of scans	256

【Results and Discussion】

<FT-IR measurements >

The model spectrum (PP/AO-50 + PP/G4-HBP) which has no interaction between AO-50 and G4-HBP was designed by adding the spectrum of PP/AO-50 and PP/G4-HBP sample. The spectrum area between 3300 to 3800 cm^{-1} has been chosen to confirm the hydrogen bonds between AO-50 and G4-HBP (Figure 3 and 4).

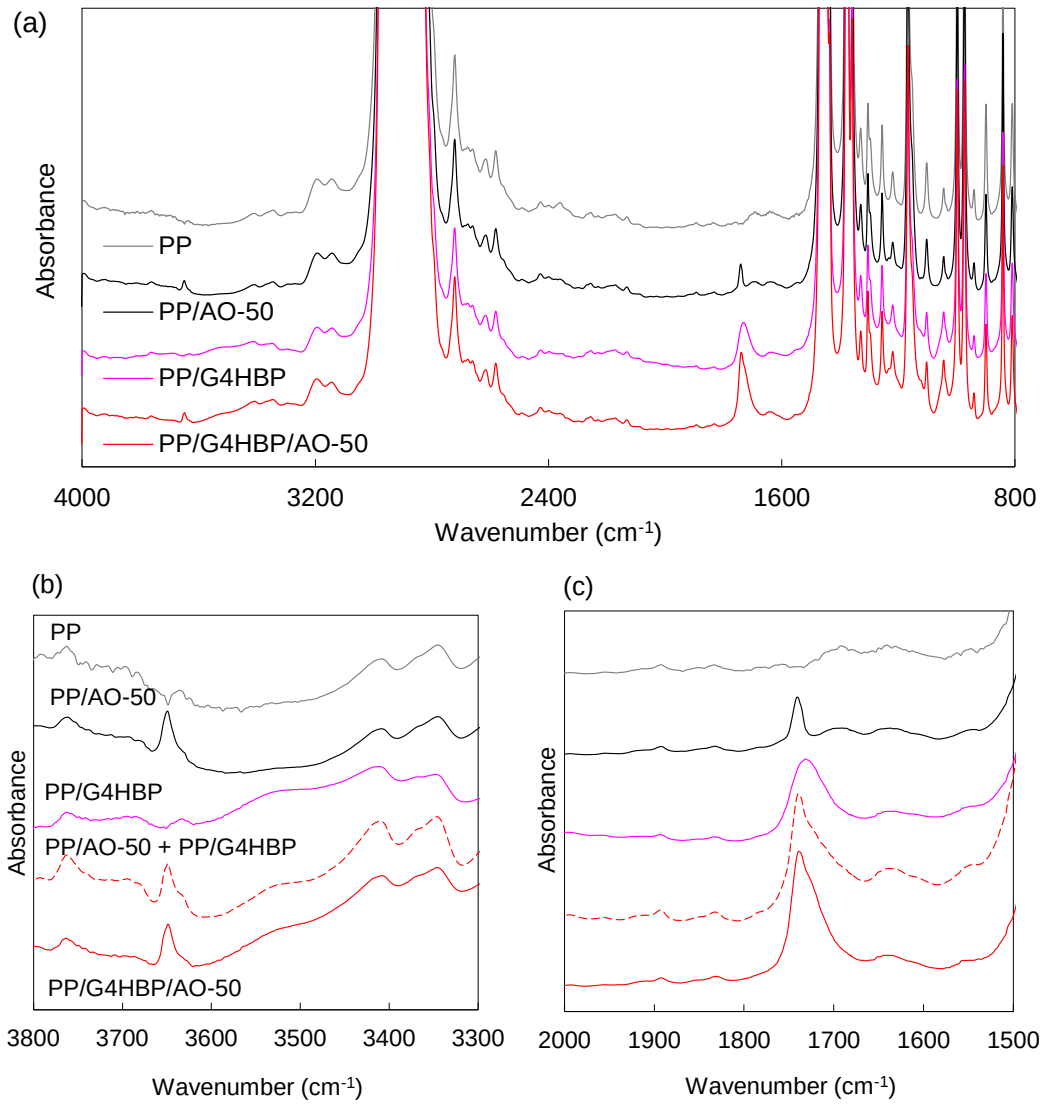

Figure 4. Infrared spectra of samples. (a) Full range spectra of samples; (b) spectra in the range from 3800 to 3300 cm^{-1} and (C) from 2000 to 1500 cm^{-1}

Hydroxyl group involved in hydrogen bonding shows the broad spectrum between 3200 to 3600 cm^{-1}. Hindered phenol has no hydrogen bonds but has free hydroxyl groups (free OH) which shows sharp peak at 3650 cm^{-1}. There must be spectrum shift and/or integration change of hydroxyl groups compared with the model spectrum (PP/AO-50 + PP/G4-HBP) if there is interaction between hindered phenol of AO-50 and hydroxyl groups (Hydrogen bonds etc.,).

PP spectrum shows no intensity related to hydrogen bonds and free hydrogens in Figure 3. PP/AO-50 spectrum shows sharp intensity free OH groups which can be assigned for hindered phenol of AO-50. On the other hand, in the case of broad intensity on peak is visible PP/G4-HBP which is related to G4-HBP ester bonds. PP/G4HBP/AO-50 shows both sharp and broaden peak.

However, the spectrum shift and integration change were not confirmed from IR results. The details of peak area are shown in Table 5 (standard peak area was decided by PP/AO-50+PP/G4-HBP).

Table 5. Peak area of free OH, Hydrogen bonded OH and ester.

	free OH	OH (Hydrogen bond)	ester
PP/AO-50+PP/G4-HBP	1.00	1.00	1.00
PP/AO-50/G4-HBP	0.97	1.05	1.00

From these results, it was found that the hydrogen bonds between AO-50 and G4-HBP were not observed in PP matrix at room temperature. However, the OIT characterization in the main research was run at 150°C. It means that the measurement

condition were different from IR conditions. In addition, it is possible that IR measurements at low temperature show low interaction between AO-50 and G4-HBP because of crystal state of AO-50 (Melting point of AO-50 is 55°C). Therefore, it is even better to run IR measurements at 150°C.

In next stage, FT-IR emission measurements were done at 150°C to observe the time dependence of interaction.

<FT-IR emission >

Figure 4 and Table 5 showed no interaction (especially hydrogen bond) between G4-HBP and AO-50 at room temperature. It was suggested that the vibration measurements should be done at same condition as OIT measurements (Chemiluminescence analysis) at high temperature. Therefore, IR measurement was also tried at high temperature (150°C) by FT-IR emission. FT-IR emission is able to run measurements with heating samples. Figure 6 shows the original data of FT-IR emission.

Pospisil, et al. examined the structure change of antioxidants during oxidation with dying PP matrix by antioxidants [6]. They reported that the main reason of the stained matrix was related to dimerization of antioxidants. In addition, they also reported the deactivated structure of antioxidants. Figure 6 shows one of the deactivated structures of AO-50.

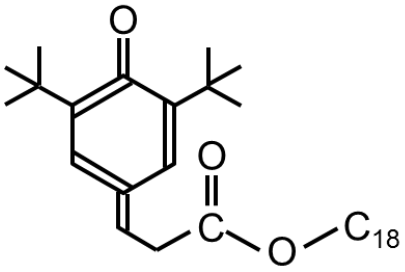

Figure 5. One of deactivated structure of AO-50

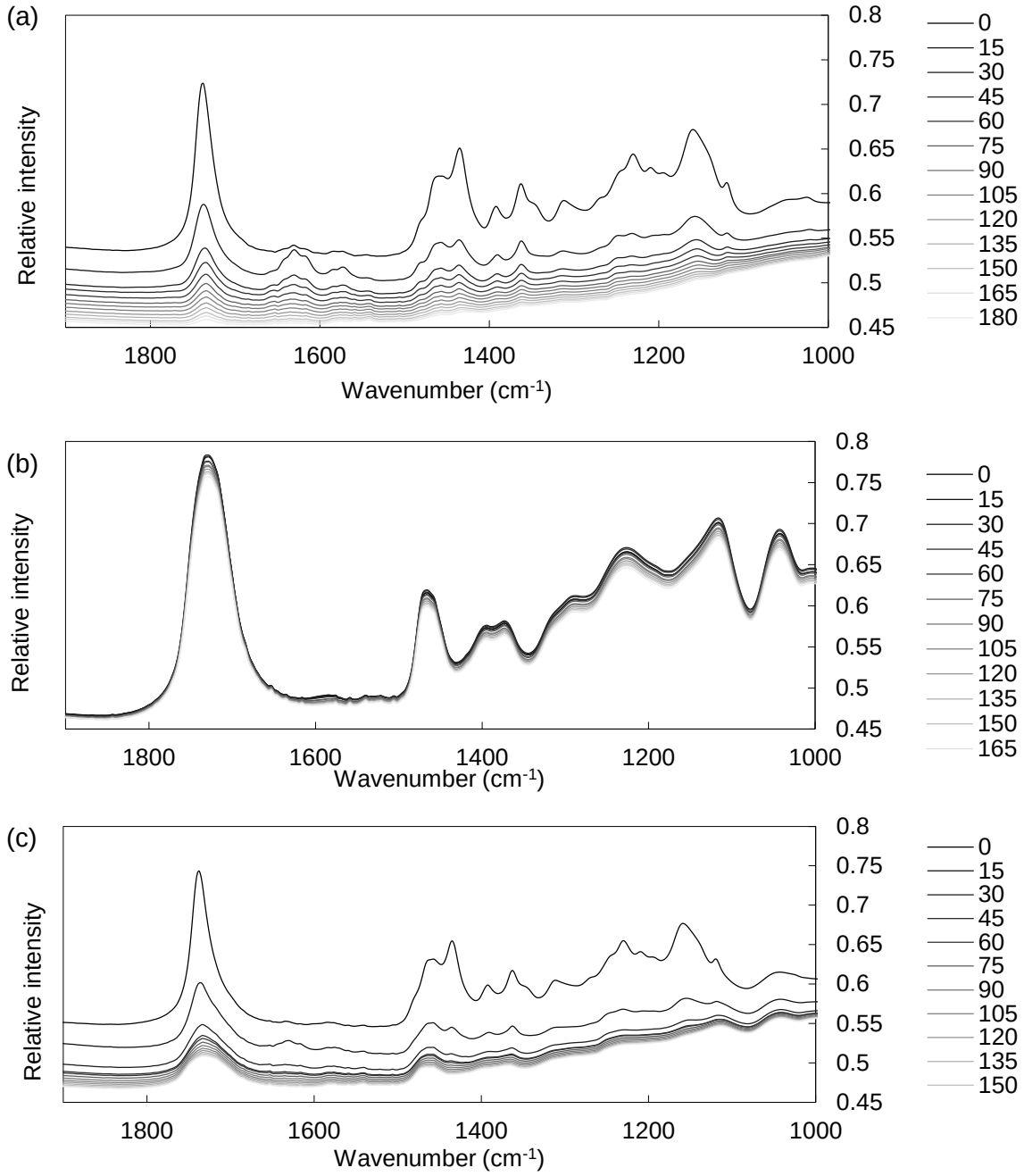

Figure 6. FT-IR emission spectra with aging time (min) at 150°C, (a) AO-50, (b) G4-HBP, (c)AO-50 with G4-HBP (1:1)

Figure 6 (a) shows the time dependence of AO-50 at 150°C. It was observed that there is a decrease of the peak intensity with increase in time. It is possible that the

decomposition and/or volatilization of AO-50 occurred during the measurements. On the other hand, G4-HBP is stable during the measurement which suggests no structural change of G4-HBP at 150°C. However, it is difficult to discuss about peak intensity with comparisons of samples in Figure 6. Figure 7 shows the modified spectra by subtraction of 180 min from original data of FT-IR emission to compare the samples with and without G4-HBP.

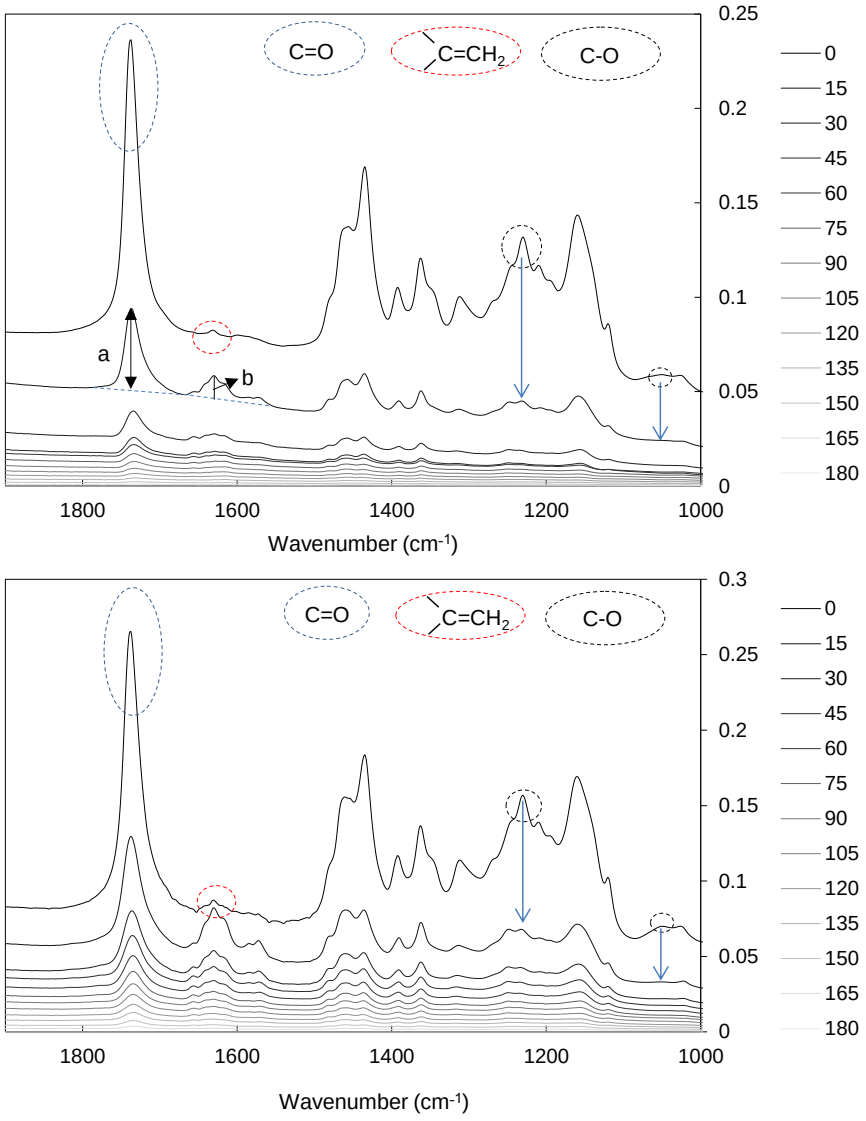

Figure 7. Spectrum of FT-IR emission of AO-50 subtracted by peak (180 min) (upper) with G4-HBP (below) without G4-HBP

It was confirmed that the peak intensity of 1630 cm^{-1} was increased at 15 min. It strongly suggested that some chemical changes of AO-50 happened in this term. This 1630 cm^{-1} peak related to carbon double bond (C=C) suggests the deactivation of AO-50 like Figure 5. In addition, the peaks intensity of 1050 cm^{-1} and 1240 cm^{-1} which come from ester bond (C=O) of AO-50 also became weaker. Therefore, the decomposition of ester bonds at ester bond of AO-50 is also highly possible. It also should be consider about the peak of 1740 cm^{-1} come from ester bonds of AO-50. The intensity of 1740 cm^{-1} peak which is being decreased over time suggests that AO-50 still remained without decomposition of itself. From these results, it is concluded that not only the decomposition of AO-50 but also volatilization of AO-50 occurred at the same time during the sample measurements.

Figure 8 shows the deactivation rate of AO-50 with and without G4-HBP with aging time at 150°C to discuss about the stabilization mechanism by G4-HBP. Deactivation rate was defined by dividing 1630 cm^{-1} peak related to C=C (deactivated peak) by 1740 cm^{-1} peak related to ester bond (unreacted AO-50 peak).

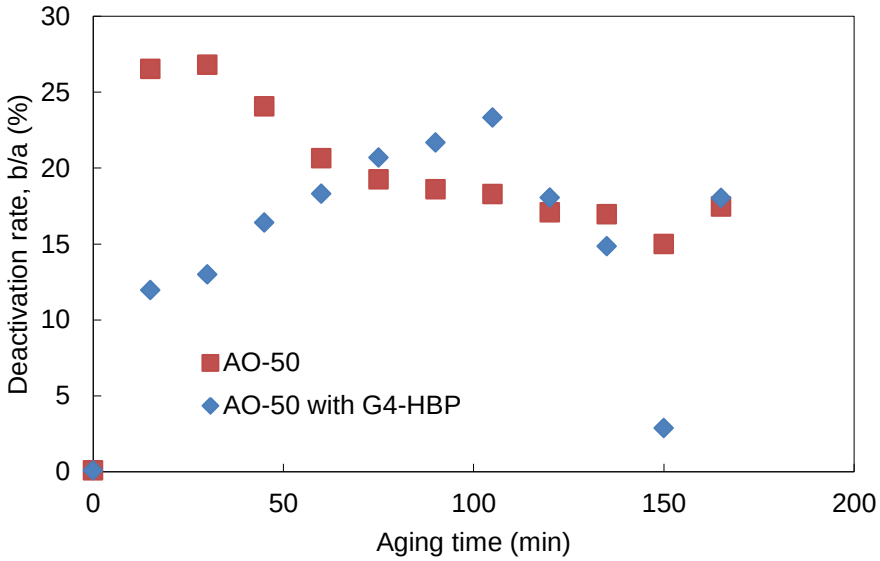

Figure 8. Deactivation rate (b/a) of AO-50 with/without G4-HBP

The sample added to G4-HBP shows lower deactivation rate in early stage (less than 60 min) than without G4-HBP in Figure 8. And then, value of deactivation rate with G4-HBP was inversely changed without G4-HBP sample at 75 min.

It was suggested that G4-HBP suppressed the deactivation of AO-50 in early stage of sample aging. Generally, the suppressing degradation of PP materials in early stage is more important than latter stage in order to get long term stabilization of PP materials because it is related to limit the expansion of degradation. As a result, one of the stabilization mechanisms by adding HBP became clear.

【Conclusion】

Vibration spectroscopic analysis for stabilization mechanism by hyperbranched polymer was focused in this minor research. The interaction between antioxidant (AO-50) and hyperbranched polymer (G4-HBP) was not observed by IR measurements at room temperature. However, the suppression of antioxidant decomposition was confirmed by FT-IR emission at 150°C. It is suggested that one of stabilization mechanism arises from suppression of antioxidants decomposition by hyperbranched polymer.

【References】

[1] M. Blumberg, C. R. Boss, J. C. W. Chien, *J. Appl. Polym. Sci*., **1965**, *9*, 3837.

[2] J. Holcik, M. Karvas, D. Kassovicova, J. Durmis, *Euro. Polym. J*., **1975**, *12*, 173.

[3] T. Taniike, M. Umemori, H. Chiba, K. Takeuchi, M. Terano, *J. Mater. Life. Soc*., **2012**, *24*, 102.

[4] T. Taniike, *Japan Patent*, 091607, **2011**.

[5] G. A. George, M. Celina, A. M. Vassallo, P. A. Cole-Clarke, *Polym. Deg. Stab*., **1995**, *48*, 199.

[6] J. Pospisil, W.-D. Habicher, J. Pilar, S. N espurek, J. Kuthan, G.-O. Piringer, H. Zweifel, *Polym. Deg. Stab*., **2002**, *77*, 531.

Acknowledgments

I would like to express my sincere regards and gratitude to Professor Graeme A. George for his invaluable guidance and support. This work would never have been performed without his help.

I would like to extend my special thanks to Dr. John M. Colwell and Dr. Melissa A.L. Nikolic for their constant help in my experiments. I pay my heartiest thanks to Dr. Llew Rintoul and also Professor Steven E. Bottle.

I am greatly thankful to all the colleagues of George Laboratory for their biggest support and encouragement. I am also grateful to Dr. Chun-Liang Yeh for being the best colleague and for his immense cooperation during my stay in Brisbane.

Finally, I am grateful to Professor Minoru Terano and Associate Professor Dr. Toshiaki Taniike.

Ikki Katada

Terano Laboratory,

School of Materials Science,

Japan Advanced Institute of Technology